Monthly Notices
of the
ROYAL ASTRONOMICAL SOCIETY

MNRAS **444,** 1125–1143 (2014) doi:10.1093/mnras/stu1385

Galaxy formation as a cosmological tool – I. The galaxy merger history as a measure of cosmological parameters

Christopher J. Conselice,[1⋆] Asa F. L. Bluck,[2] Alice Mortlock,[1,3] David Palamara[4,5] and Andrew J. Benson[6]

[1]*School of Physics & Astronomy, University of Nottingham, Nottingham NG7 2RD, UK*
[2]*Department of Physics and Astronomy, University of Victoria, Victoria, BC V8P 1A1, Canada*
[3]*Institute for Astronomy, University of Edinburgh, Royal Observatory, Edinburgh EH9 3HJ, UK*
[4]*School of Physics, Monash University, Clayton, VIC 3800, Australia*
[5]*Monash Center for Astrophysics (MoCA), Monash University, Clayton, VIC 3800, Australia*
[6]*Carnegie Observatories, 813 Santa Barbara Street, Pasadena, CA 91101, USA*

Accepted 2014 July 8. Received 2014 July 8; in original form 2013 December 4

ABSTRACT

As galaxy formation and evolution over long cosmic time-scales depends to a large degree on the structure of the universe, the assembly history of galaxies is potentially a powerful approach for learning about the universe itself. In this paper, we examine the merger history of dark matter haloes based on the Extended Press–Schechter formalism as a function of cosmological parameters, redshift and halo mass. We calculate how major halo mergers are influenced by changes in the cosmological values of $\Omega_{\rm m}$, Ω_Λ, σ_8, the dark matter particle temperature (warm versus cold dark matter), and the value of a constant and evolving equation of state parameter $w(z)$. We find that the merger fraction at a given halo mass varies by up to a factor of 3 for haloes forming under the assumption of cold dark matter, within different underling cosmological parameters. We find that the current measurements of the merger history, as measured through observed galaxy pairs as well as through structure, are in agreement with the concordance cosmology with the current best fit giving $1 - \Omega_{\rm m} = \Omega_\Lambda = 0.84^{+0.16}_{-0.17}$. To obtain a more accurate constraint competitive with recently measured cosmological parameters from *Planck* and *Wilkinson Microwave Anisotropy Probe* requires a measured merger accuracy of $\delta f_{\rm m} \sim 0.01$, implying surveys with an accurately measured merger history over 2–20 deg^2, which will be feasible with the next generation of imaging and spectroscopic surveys such as *Euclid* and LSST.

Key words: galaxies: evolution – galaxies: formation – galaxies: structure.

1 INTRODUCTION

One of the major goals in science is determining the past history and future evolution of the universe. The determination of this in a quantitative way has a long history, starting with the work of Hubble (1929) who determined that the universe was expanding based on radial velocity and distance measurements of galaxies. This has continued using various approaches, including the use of cosmic microwave background (CMB) measurements, with the most recent work using e.g. *Wilkinson Microwave Anisotropy Probe* (*WMAP*), *Planck* and BICEP2 (e.g. Komatsu et al. 2011; Ade et al. 2013, 2014). Currently, the use of the CMB and Type Ia supernova are the most common and influential methods for measuring cosmological parameters (e.g. Kessler et al. 2009), along with baryonic acoustic oscillations and clustering measurements (e.g. Eisenstein et al. 2005; Blake et al. 2011).

One of the dominant features of the current popular cosmological model is that the universe's energy budget is perhaps dominated by a cosmological constant – the so-called dark energy. The major evidence for this dark energy is largely based on observations of the luminosities of supernova at various redshifts (e.g. Riess et al. 1998; Perlmutter et al. 1999). Other evidence for dark energy comes from baryonic acoustic oscillations (e.g. Eisenstein et al. 2005), and fluctuations in the cosmic background radiation (e.g. Komatsu et al. 2011). The major result of this is that the universe appears to be accelerating since $z < 1$, and perhaps undergoes a deceleration phase at higher redshifts (Riess et al. 2004).

What is currently lacking within this cosmological paradigm is physical evidence for the existence of dark energy, which in

⋆ E-mail: conselice@nottingham.ac.uk

principle can significantly change the evolution of the constituents of the universe, of which galaxies are the fundamental component. The basic idea is that if the universe is undergoing an acceleration phase, then the rate of structure formation will decline with time, halting the growth of massive structures, such as galaxy clusters (e.g. Allen et al. 2004; Vikhlinin et al. 2009). In fact, observations of the number densities of galaxy clusters can be used as an alternative method for constraining dark energy properties (e.g. Vikhlinin et al. 2009).

Recently, with a basic but firm understanding of galaxy formation and evolution it is now possible to go beyond observations of clusters, supernova and the cosmic background radiation to use galaxies themselves as a new probe of cosmology. We explore in this paper how cosmological properties affect the formation of galaxies throughout their history based on examining the formation histories of dark matter haloes. This lets us examine both how galaxy formation can be used as a probe of cosmology, and how cosmology affects the formation of galaxies. In this sense the formation history of galaxies in the universe is potentially another probe of the energy and kinematics of the universe.

The use of galaxies for cosmology is not a new idea, and early attempts to measure cosmological properties, largely the measurement of the Hubble constant, relied on luminosities and properties of stars and globular clusters in external galaxies. Several cosmological tests were also proposed in the 1920–1930s that used the angular sizes, counts and surface brightness evolution of galaxies (e.g. Tolman 1930; Sandage 1988). However, these approaches were largely abandoned once it was realized that galaxies evolve significantly through time, and that the properties of nearby galaxies are not necessarily the same as more distant galaxies.

Since we are now becoming confident in the measurements of galaxy properties, and how at least massive galaxies evolve and form over time, especially since $z \sim 3$ (e.g. Bluck et al. 2012; Conselice et al. 2013; Muzzin et al. 2013) we are in a position to reevaluate whether galaxy properties, and their evolution, can be used to determine features of the Universe. While early cosmological investigations were based on measuring the Hubble constant through the distance–velocity relation, and later through trying to measure the value of the deceleration parameter, q_0, new approaches using the evolution of galaxy properties can potentially be used to derive features of the dominant cosmological paradigm.

We specifically investigate in this paper whether the evolution of galaxies is consistent with the currently accepted ideas concerning a Λ-dominated universe with a transition from deceleration to acceleration occurring sometime around $z \sim 0.7$ (Turner & Riess 2002). The fact that the universe may transition from one which is decelerating to one which is accelerating may have a profound impact on the formation history of galaxies which would otherwise be different in a universe with a different cosmology. The idea behind this paper is that the history of galaxy assembly is driven by cosmological parameters, and one of the ways this can be seen is through the merger history.

In this first paper of this series, we investigate this problem by comparing models of halo and galaxy formation, which vary as a function of cosmology and dark matter properties, to the observed galaxy merger history. We investigate the possibility that comparisons between halo merger histories and observed galaxy mergers can be used as an independent new measurement of cosmological properties, and give us some indication of what would be necessary to use these features to constrain cosmology more directly using future telescopes and space missions. To do this, we also discuss how comparing observations of galaxies to dark matter haloes is perhaps a better approach for understanding bulk galaxy formation than to rely on the simulations of galaxy formation themselves.

We furthermore show how comparisons between the galaxy merger history predicted in cold dark matter (CDM) simulations differ depending on the underlying dark matter. We demonstrate that the temperature of the dark matter particle also can have a fundamental influence on the predicted galaxy merger history. We further conclude how comparing halo merger models to observed galaxy mergers can reveal clues to the selection of observed mergers and how, and whether, there is a self-consistent observational and cosmological based theoretical picture for the formation history of galaxies.

This paper is organized as follows: Section 2 gives a description of the models we use in this paper, Section 3 includes a discussion of the results of an analysis of halo merger histories. Section 4 is a description of the comparison between galaxy merger history predictions, the actual merger history, and consists of our main analysis, Section 5 is a discussion of the implications for these results Section 6 is a discussion of our results and Section 7 is our summary. We refer to a cosmology with $\Omega_{\rm m} = 0.3$, $\Omega_\Lambda = 0.7$; $\sigma_8 = 0.9$; $H_0 = 70$ km s^{-1} Mpc^{-3} as the concordance cosmology.

2 DARK MATTER HALO MODELS

2.1 Formalism

In the dominant theory for galaxy formation, based on a ΛCDM cosmology, galaxies assemble by merging with one another over time (e.g. White & Rees 1978). The basis for this merging is the dark matter assembly history, and how dark matter halo masses grow by merging with one another. Using Newtonian dynamics plus a simple expanding universe model, it is now possible to predict the total halo mass functions of galaxies across a large range in mass to within 5 per cent, comparing different computer simulation results. With the small discrepancies based on the differences between methods of the various calculations rather than fundamental physics (e.g. Reed et al. 2007). In particular, different group finding algorithms are largely the cause of the small differences in masses, rather than fundamental physics (e.g. Kneber et al. 2013).

Predictions for how structure assembles are the backbone of any theory of galaxy formation. Since galaxies are believed to form at the cores of dark matter haloes, then the formation of galaxies should follow in some way how the dark matter assembles. Dark matter haloes and large-scale structure are created through these haloes hierarchically. This process can be predicted based on the basic physics of gravitational collapse of matter in an expanding universe, and its later evolution, and therefore does not involve uncertain baryonic physics. The details of how dark matter haloes assemble is now predicted in detailed *N*-body and semi-analytical simulations (e.g. Fakhouri & Ma 2008). These simulations essentially predict when two existing dark matter haloes merge together to form a large halo within the standard ΛCDM cosmologies assumed.

It is fairly straightforward to use simulations of structure formation to predict how dark matter haloes with descendant masses between 10^{12} M$_\odot$ $< M_{\rm halo} <$ 10^{15} M$_\odot$ assemble with time (e.g. Fakhouri & Ma 2008). We investigate in this paper what various models predict for halo mergers. Our primary method is to use a generalized code for calculating dark matter halo mergers within a given cosmology. To do this, we calculate the merger history for dark matter haloes through using the 'GROWL' algorithm by Hamilton (2001) using a power spectrum calculated by Eisenstein & Hu (1999). Using this numerical formalism, it is possible to determine

the assembly history of dark matter haloes using basic gravitational collapse physics.

To calculate this, we use the results of Hamilton (2001), and a modified form of the GROWL code to compute the linear growth factor

$$g = \frac{D}{a} \tag{1}$$

for structure in the universe as a function of time, where D is the amplitude of the growth mode, and a is the scale factor. The linear growth rate,

$$f = \frac{\mathrm{dlnD}}{\mathrm{dln}\,a} \tag{2}$$

is the derivative of g, and relates to peculiar motions within the universe. Using a Friedmannn–Robertson–Walker universe, the growth factor g can then be written as

$$g(\Omega_m, \Omega_\Lambda) = \frac{D}{a} = \frac{5 \times \Omega_\mathrm{m}}{2} \int_0^1 \frac{\mathrm{d}a}{a^3 H(a)^3}, \tag{3}$$

where a is the scale factor normalized to unity, and $H(a)$ is the Hubble parameter normalized to unity when $a = 1$, where

$$H(a) = (\Omega_\mathrm{m} a^{-3} + \Omega_\mathrm{k} a^{-2} + \Omega_\Lambda)^{1/2}. \tag{4}$$

The value of the growth factor and the Hubble constant $H(a)$ depend upon the value of cosmological parameters. The linear growth rate f can then be written as

$$f(\Omega_\mathrm{m}, \Omega_\Lambda) = -1 - \frac{\Omega_\mathrm{m}}{2} + \Omega_\Lambda + \frac{5\Omega_\mathrm{m}}{2g}. \tag{5}$$

Analytical solutions to the above growth rate are presented in detail in Hamilton (2001) for different cosmological parameter ratios. The GROWL code then implements these fitting formula for various scenarios to predict what the growth factor is during the history of the universe, as a function of cosmology and time.

The power spectrum used within this code originates from Eisenstein & Hu (1999), who calculate fitting formula for the matter transfer function as a function of wavenumber, time, the massive neutrino density, number of neutrino species, the Hubble parameter today, the cosmological constant, baryon density and the spatial curvature. Mergers occur via the set excursion methodology from Press & Schechter (1974) but using the extended formalism. As a result, we measure the halo merger history as a function of the mass ratio of the halo mergers:

$$\eta = \frac{M_2 - M_1}{M_2}, \tag{6}$$

where M_2 is the sum of the halo masses of the two merger components (or the resulting halo mass) and M_1 is the halo mass of the more massive progenitor.

We use these models with a variety of different cosmological parameters to investigate how the halo merger history varies with cosmology. The cosmological parameters that we vary are the matter density Ω_m, the dark energy density Ω_Λ, the neutrino density Ω_μ, the Hubble constant, H_0, the baryonic density Ω_B, the temperature of the CMB T_CMB, the number of neutrino species, N_ν, value of σ_8 and the spectral index n. We define the cosmology henceforth as the quantity

$$\Theta = \left(\Omega_\mathrm{m}, \Omega_\Lambda, \Omega_\mu, H_0, \Omega_\mathrm{B}, T_\mathrm{CMB}, N_\nu, \sigma_8, n\right). \tag{7}$$

Our method uses an altered version of the publicly available GROWL code. We measure the halo merger history through a particular type of 'major' halo merger. These cosmological based halo mergers are designed to match as much as possible the merger criteria used to find mergers occurring in actual galaxies (Section 2.2). We use these halo mergers as our primary method for comparing with observable galaxy mergers, as we show in Section 4 that the predicted galaxy merger history is currently too uncertain to be used to compare with real galaxies to derive cosmology, but that the halo mergers are known accurately enough to make this comparison.

2.2 Merger fraction calculation and time-scales

In this paper, we only discuss mergers which are major for both the observational data and the theoretical calculations. The criterion for finding a major merger is that a halo at a given redshift must have had a merger with another halo of mass 1:4 or less within the past ∼0.4 Gyr. This is the same criterion we use to find mergers in galaxies based on pairs separated by 30 kpc (e.g. Bluck et al. 2012), and when using the structural CAS system (e.g. Conselice, Yang & Bluck 2009; Conselice 2014). This also matches well the mass ratio and time-scales for mergers for the CAS parameters (e.g. Lotz et al. 2011). We later discuss how these merger fractions would change if using a different value of the merger time-scale and after matching halo versus stellar mass ratio mergers.

We use a merger time-scale of 0.4 Gyr throughout this paper, as this is the average time-scale in which we are sensitive to within the observations based on both N-body models (Conselice 2006b; Lotz et al. 2008a), and when examining the empirically measured merger time-scales (Conselice 2009). Below we discuss in detail the reasoning behind this, and the uncertainties associated with using a fixed time-scale.

First, it is clear that numerical models of massive galaxy mergers give an average time-scale of ∼0.4 Gyr. For example, Conselice (2006b) and later Lotz et al. (2008a, 2010a,b) investigate the location of different phases of various types of mergers in morphological parameter space. They use these models to calculate the time-scales for how long these simulated galaxies appear as a 'merger', based on where they fall in these non-parametric structural spaces. While Conselice (2006b) used only dark matter simulations, the Lotz et al. studies investigate the stellar distribution and how dust, viewing angle, orbital parameters, gas properties, SN feedback and total mass alter the merger time-scale (e.g. Lotz et al. 2010b; Moreno et al. 2013). It is found in these papers that very few properties beyond mass ratio and gas mass fraction affect the derived merger time-scales.

These simulations show that mergers are identified within both CAS at the first pass of the merger, as well as when the systems finally merge together to form a remnant (Lotz et al. 2008). However, merging galaxies are not found in the merger area of the non-parametric structural parameters for the entire merger, as was found by Conselice (2006b). This however allows the time-scales for structural mergers to be calculated. Lotz et al. (2008, 2010a) find that the asymmetry time-scales for gas-rich major mergers are 0.2–0.6 Gyr and 0.06 Gyr for minor mergers (Lotz et al. 2010a). While the individual time-scale for a pair of galaxies within a dark matter halo to merge will vary, based on the variety of models the average is 0.4 Gyr and we use this throughout this paper as our measured merger time-scale.

An issue that we have to address is that these time-scales are for gas-rich mergers, and would not necessarily apply for gas-poor or dry mergers. However, at the redshifts we are investigating here, nearly all galaxy mergers will have some gas, as pure dry mergers are relatively rare (e.g. Lin et al. 2008; Conselice et al. 2009; De Propris et al. 2010). Furthermore, the massive galaxies that we examine in

this paper have gas fractions which are on average ∼10 per cent at $z = 1$–3, with little variation (e.g. Mannucci et al. 2009; Conselice et al. 2013). Therefore, it is unlikely that the computed merger time-scales differ due to a lack or overabundance of gas. We however do calculate how our merger fractions would change if using a different time-scale. In summary, if our observed mergers have a longer/shorter time-scale then the resulting comparisons for halo mergers would be higher/lower.

We utilize these numerical models to determine the fraction of haloes which have merged within our given time-scale. For our purposes we determine the merger fraction of haloes, which we denote as $f_{\rm halo}$, at a variety of redshifts.

$$f_{\rm halo} = \frac{N_{\rm merger}(M_{\rm halo}, \eta, z, \tau, \Theta)}{N_{\rm tot}(M_{\rm halo}, \eta, z, \tau, \Theta)}. \quad (8)$$

Later we investigate how the merger history of haloes, and the value of $f_{\rm halo}$ changes as a function of different values of the equation of state parameter ω, and for a varying $\omega(z)$ as a function of redshift. These calculations originate from the GALACTICUS code of Benson (2012). Within our calculations of the merger fraction we also take into account double mergers whereby a halo or galaxy undergoes more than one merger in a given time-scale. The merger fraction includes the total number of mergers the examined population (selected by mass in this case) undergoes divided by the total number of galaxies in that selection. Therefore, if a single galaxy/halo undergoes more than a single merger it is accounted for explicitly.

GALACTICUS is a semi-analytic model which is easily adapted to differing physical and initial conditions. We utilized the same framework presented in the Hamilton (2001) structure formation model, but through using an equation of state parameter, ω, as well as through the use of an evolving form as a function of redshift ($\omega(z)$).

We also use the results from the Millennium simulations (Springel et al. 2005) for both the merger history of galaxies which was discussed in depth in Bertone & Conselice (2009), as well as the merger history of haloes. We furthermore compare with warm dark matter (WDM) semi-analytical models from Menci et al. (2012) to test how different dark matter particle temperatures can affect the galaxy merger history. Finally, we also compare with abundance matched merger histories from Hopkins et al. (2010).

2.3 Data sources

One of the major goals of this study is to compare the observed galaxy merger history with predictions from simulations for the halo and predicted galaxy merger history. As such, the data we use for this comparison are from a diversity of sources and different surveys of distant galaxies. Most of these are deep *Hubble Space Telescope* imaging surveys which have accurately measured stellar masses, redshifts and merger fractions out to these redshifts.

The galaxy merger data we use in this study come from several studies of the merger history using the CAS structural method (Conselice 2003, 2014), as well as galaxies in pairs (Bluck et al. 2009, 2012; Lopez-Sanjuan et al. 2010; Man et al. 2012). The surveys we take our merger data from include the GOODS NICMOS Survey (Conselice et al. 2011), NICMOS imaging of the COSMOS field (Man et al. 2012), and the Hubble Ultra Deep and Deep Fields (e.g. Williams et al. 1996; Conselice, Rajgor & Myers 2008). We also take results from Bluck et al. (2009, 2012) for $M_* > 10^{11}$ M$_\odot$ galaxies from the GOODS NICMOS Survey to $z = 3$ (Mortlock et al. 2011). For the most massive galaxies with $M_* > 10^{11}$ M$_\odot$ at $z < 3$ we supplement our data with pair fractions taken from the Ultra Deep Survey (UDS) when fitting with models. The other previous studies we use for comparison are those from Conselice et al. (2008, 2009) who computed the merger history for observed galaxies based on data observed in the *Hubble Ultra Deep Field*, and the COSMOS and EGS fields for systems at $z < 1.5$. We also use new Cosmic Assembly Near-infrared Deep Extragalactic Legacy Survey (CANDELS) observations of the merger history from asymmetries calculated within the CANDELS area of the UDS field (Mortlock et al. 2013).

There are many other potential merger histories that we can use, but do not, due to time-scale and major/minor merger sensitivity, we only use galaxies in pairs and those measured with the CAS system, which has a well-defined merger time-scale for gas-rich major mergers discussed in Section 2.2. When examining the merger fraction history it is clear that there are significant differences between the various methods of measuring mergers (e.g. Conselice et al. 2009; Lotz et al. 2011). This is due to different methods being sensitive to various time-scales of the merger process as well as to the mass ratios of mergers.

We are interested in a specific type of merger in this paper – systems which are merging and which have a progenitor mass ratio of 1:4 or lower and have merged within the past 0.4 Gyr. Detailed simulations from Conselice (2006) and Lotz et al. (2010a) show that a positive merger signature is seen when the mass ratio is 1:4 in total mass. We also make sure to investigate the corresponding stellar mass ratios, based on the dark matter halo merger ratio, when comparing predicted halo merger fractions to observed pair fractions (Section 5.2). We therefore only use the CAS mergers which have this time-scale sensitivity (e.g. Conselice 2006; Lotz et al. 2008), and pairs of galaxies where the merger mass ratio can be measured directly and where pairs with separations of <30 kpc mergers have a similar time-scale as the CAS selected mergers (e.g. Conselice et al. 2009; Bluck et al. 2012) of about $\tau = 0.4$ Gyr. We also utilize these studies as they use similar or the same methods to calculate photometric redshifts and stellar masses allowing us to minimize these sources of uncertainty between various results.

The stellar masses we use to constrain our observed sample originate from fitting observed Spectral Energy Distributions (SEDs) to stellar population synthesis methods. The procedure for this differs between the various studies, but the results are largely consistent, and are normalized such that they use the same initial mass function (Salpeter), and the same range of stellar ranges from 0.1 to 100 M$_\odot$. The fitting method for our stellar masses consists of fitting a grid of model SEDs constructed from Bruzual & Charlot (2003, hereafter BC03) stellar population synthesis models, using a variety of exponentially declining star formation histories, with various ages, metallicities and dust contents included. The models we use are parametrized by an age, and an e-folding time for parameterizing the star formation history, where SFR(t) $\sim$ e$^{-t/\tau}$.

The values of τ are randomly selected from a range between 0.01 and 10 Gyr, while the age of the onset of star formation ranges from 0 to 10 Gyr. The metallicity ranges from 0.0001 to 0.05 (BC03), and the dust content is parametrized by $\tau_{\rm v}$, the effective V-band optical depth for which we use values $\tau_{\rm v} = 0$, 0.4, 0.8, 1.0, 1.33, 1.66, 2, 2.5, 5.0. Although we vary several parameters, the resulting stellar masses from our fits do not depend strongly on the various selection criteria used to characterize the age and the metallicity of the stellar population.

We also utilize photometric and spectroscopic redshifts for our measurements of the stellar masses which also come into play when measuring the evolving merger history. The typical photometric redshift accuracy for these surveys is quite good, with values of $\delta z/(1 + z) \sim 0.03$ (Hartley et al. 2013; Mortlock et al. 2013).

Details of how these photometric redshifts are computed are included in the above cited papers (e.g. Conselice et al. 2009; Mortlock et al. 2011, 2013; Bluck et al. 2012). The errors in the merger fractions which we later use to fit to the predicted halo and galaxy mergers fully take into account the uncertainties in the stellar masses and redshifts for these samples. This is in fact the largest source of uncertainty when calculating the most likely cosmological model based on the merger fraction evolution.

3 HALO AND GALAXY MERGER PREDICTIONS

In the following sections, we investigate the halo and galaxy merger histories both predicted, for haloes (Sections 3.1– 3.3), and in Section 4 for the observed galaxies. In this paper, we discuss many observed and predicted galaxy and halo mergers. To simply things, we give a brief overview here of what is presented later. In this section, we only discuss halo mergers, and how they evolve as a function of halo mass, redshift and cosmology. These halo mergers are the basis for the rest of the paper. We give a detailed description of the halo merger history within the ΛCDM framework, comparing with predictions from semi-analytical models based on the Millennium simulations I and II, as well as with halo occupation distribution (HOD) modelling predictions.

In Section 4, we discuss the observed and predicted merger history for galaxies at a given stellar mass selection using several methods and simulations (e.g. Bertone & Conselice 2009; Hopkins et al. 2010). Section 4.1 gives an overview of the observed galaxy merger history which we later compare the halo mergers described in this section. Section 4.2 is a discussion of the latest in galaxy merger history predictions from both semi-analytical models and abundance matching. We describe there how the predicted galaxy mergers are unable to match data as well as the dark matter haloes themselves, and therefore we use a methodology to compare directly the halo mergers to the observed galaxy mergers in Section 5.

3.1 Halo mergers as a function of redshift and mass

We first describe the merger histories of haloes using the concordance cosmology, defined as $\Omega_\Lambda = 0.7$, $\Omega_m = 0.3$ and $\sigma_8 = 0.9$, as a function of halo mass. The merger histories for galaxy haloes has been studied previously, but mostly only within the standard cosmology. Early results (e.g. Gottlober, Klypin & Kravtsov 2001) found that the merger history for haloes can be described as a power-law increase with redshift as $\sim(1+z)^3$. More detailed predictions have been provided by modern simulations such as the Millennium simulation (e.g. Fakhouri & Ma 2008; Bertone & Conselice 2009; Fakhouri, Ma & Boylan-Kolchin 2010; Hopkins et al. 2010) where both the merger history for haloes and galaxies are simulated and predicted. These simulations find that the merger history of haloes increases as a power law (e.g. Fakhouri & Ma 2008). These simulations also find that galaxy mergers are less common than halo mergers, and that the predicted galaxy merger fraction is much lower than what is observed (e.g. Conselice et al. 2003; Bertone & Conselice 2009; Jogee et al. 2009; Hopkins et al. 2010).

However, there is a better match between galaxy mergers and haloes when using HOD models which match dark matter haloes predicted to exist at a given redshift to observed galaxies selected by stellar mass and clustering (e.g. Hopkins et al. 2010). In this case, the galaxy merger fraction based on stellar mass is determined by the merger fraction of the haloes in which these galaxies are located (Section 4.2).

3.1.1 Redshift evolution

Here, we investigate the predicted merger history for haloes using the basic CDM model predictions with the methods outlined in Section 2. The predicted merger histories of haloes of a given halo mass limit (M_{halo}) using the formalism from Section 2 are shown in Fig. 1 for a standard ΛCDM cosmology. We select these haloes through minimum halo mass cuts, and show results for systems with log $M_{halo} > 9$ up to log $M_{halo} > 13$. We only investigate here, as explained in detail in Section 2, the merger fraction for these haloes of a given mass which merged with another halo, with a mass at least a fourth of the mass of its halo, and within 0.4 Gyr.

Fig. 1 shows a general trend such that the merger fractions of haloes are very high in the early universe, up to redshifts $z \sim 6$, with haloes of the highest masses at $M_{halo} > 10^{13}$ $M_\odot$ having a merger fraction close to $f_{halo} \sim 1$. Our predictions for the halo merger history within the mass ranges where galaxies are found agree with those predicted in the Millennium simulations I and II (Fakhouri et al. 2010), and within the merger simulations of Stewart et al. (2009). We also show the predicted quantities for predicted galaxy mergers as the lower line with points in Fig. 1, based on the Millennium simulation, demonstrating the much lower values for galaxies than haloes in the same simulation (Section 4).

We parametrize these halo merger histories as a power law of the form (e.g. Bluck et al. 2009, 2012),

$$f_{halo}(z, M_{halo}) = f_{halo}(0, M_{halo}) \times (1+z)^m, \quad (9)$$

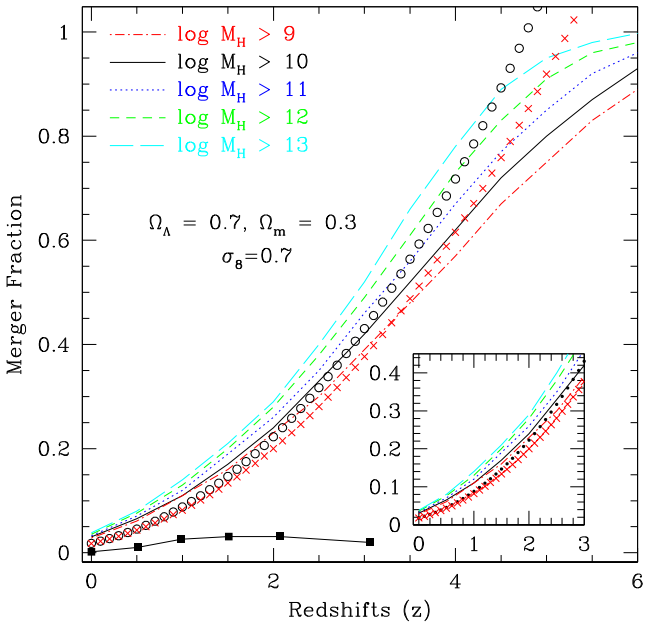

Figure 1. The halo merger history for galaxies of a given halo mass in the concordance cosmology, with the lines for the different halo masses defined on the upper left. The halo merger fraction plotted here is the fraction of galaxies at a given halo mass which has merged with another halo of at least a factor of 0.25 or greater than the mass of the progenitor halo, and within the past 0.4 Gyr. The inset shows the detailed merger history for the same systems at $z < 3$. We also show as the line with open circles the best-fitting power law to the merger history from the Millennium simulation (e.g. Fakhouri et al. 2010). Furthermore, the lower solid line with box points is the Millennium simulation prediction for galaxy mergers (as opposed to halo mergers) with log $M_* > 10$. The red crosses are model predictions from Stewart et al. (2009) for galaxies with halo masses of $M_{halo} = 10^{12}$ $M_\odot$.

Table 1. The best-fitting power-law fits from equation (9) to the merger history for dark matter haloes using haloes of different masses. These merger histories are listed at the halo mass $M_{\rm halo}$ limit. These fits are for the merger history up to $z = 4$.

Mass limit	f_0	m
$\log M_{\rm halo} > 9$	0.030 ± 0.001	1.85 ± 0.03
$\log M_{\rm halo} > 10$	0.029 ± 0.001	1.94 ± 0.03
$\log M_{\rm halo} > 11$	0.033 ± 0.001	1.88 ± 0.03
$\log M_{\rm halo} > 12$	0.030 ± 0.001	1.91 ± 0.01
$\log M_{\rm halo} > 13$	0.036 ± 0.001	1.92 ± 0.03

where $f_{\rm halo}(z = 0, M_{\rm halo})$ is the halo merger fraction at $z = 0$ and m is the power-law index for the merger history. Higher values of m are fit for steeper merger fractions. Merger histories have often been fitted with these power-law forms for galaxies at various stellar mass and luminosity cuts using real data for some time, although this is one of the first times this has been done for dark matter haloes as a function of cosmology. Previously, Gottlober et al. (2001) applied this fitting method to merger histories in the standard cosmology.

We list the results of this fitting for CDM haloes of various masses in Table 1. These results show that the halo merger history is similar at $z = 0$ at all halo masses, differing by only a small amount. However, the power-law increase is such that the more massive galaxies have a steeper rise in their halo mergers, and thus a larger merger fraction at earlier times than lower mass systems. This is a demonstration of the hierarchical nature of structure formation in haloes. This is also opposite to what is seen in the galaxy population where the more massive systems appear to end their merger and formation processes before lower mass ones (e.g. Conselice et al. 2003, 2009; Bundy et al. 2006; Mortlock et al. 2011).

3.1.2 Variation with halo mass

Another remarkable aspect of Fig. 1 is that the differential between the halo mass merger histories amongst the various mass selections is smallest at the lower redshifts, and highest at $z > 4$. This shows that the merger properties for haloes of different halo masses is similar at lower redshifts, but diverges more at the highest redshifts. Therefore, the halo assembly history is more distinct earlier, as a function of $M_{\rm halo}$, rather than later, in the universe.

Currently, the observed merger history is largely limited to studies at relatively modest redshifts, those at $z < 3$ (e.g. Conselice et al. 2008, Mortlock et al. 2013; cf. Conselice & Arnold 2009). Therefore we, in particular, examine within this paper the halo merger histories given our cosmological models at these lower redshifts, limited to $z < 3$. At these redshifts, the merger fractions for haloes over four orders of magnitude in mass differ by a maximum of $\delta f_{\rm halo} \sim 0.2$.

To study this in more detail in the inset of Fig. 1, we show merger histories for haloes as a function of redshift up to $z \sim 3$. To quantify this, we fit the change in the halo merger history as a function of halo mass at two redshifts, $z = 2.5$ and $z = 1$. We later use these to determine the uncertainty in the matching of halo and stellar masses, and therefore to go from the halo merger history to the galaxy merger history. At all redshifts, we find that this relation is linear and is well described by a function of the form:

$$f_{\rm halo}(z, M_{\rm halo}) = a \times \log M_* + b. \quad (10)$$

We find for $z = 2.5$ the values $a = 0.025 \pm 0.001$ and $b = 0.08 \pm 0.01$. This is a very shallow slope, and shows that the halo merger fraction at a given redshift does not change very much between halo masses of $\log M_{\rm halo} = 9$–13. At lower redshifts, the relation becomes even flatter, with fits for $z = 1$, $a = 0.010 \pm 0.001$ and $b = 0.011 \pm 0.002$. For the remainder of the paper, we only examine the merger history out to $z = 3$ as this is currently where we have the most certainty in our ability to measure masses and the merger history in actual galaxies (Section 4).

3.2 Variation with $\Omega_{\rm m}$ and Ω_Λ

One of the features we investigate with our halo merger histories is how the merger history changes within different underlying cosmological parameters. This allows us to investigate, among other things, whether the merger history of galaxies is consistent with the dominant cosmological model. In Fig. 2, we show the merger history for haloes of masses $M_{\rm halo} > 10^{12}$ $M_\odot$ and for $M_{\rm halo} > 10^{11}$ $M_\odot$ using our prescribed method for finding and defining merging haloes (Section 2), and within the different cosmologies listed in Table 2.

What Fig. 2 shows is that the cosmology built into the structural evolution of the universe can potentially strongly alter the history of halo mergers and thus the formation of structure. The lowest merger histories are those with a cosmology which has a zero cosmological constant, and a low dark matter content. The highest merger histories are for Einstein–de Sitter cosmologies in which the total matter density is $\Omega_{\rm m} = 1$ with a zero cosmological constant (Cosmo-4 in Table 2). Furthermore, there is a clear correlation with higher merger fractions for higher values of $\Omega_{\rm tot}$. This is an indication that the merger history is tracing to some degree the geometry of the universe.

This figure however shows that even for a total density of $\Omega = 1$ there are variations within the merger history. Three extreme models are shown in Fig. 2 – one in which the energy density is completely in the form of matter (Cosmo-4; the short dashed line), one which has the currently accepted cosmological model (Cosmo-7; $\Omega_{\rm m} = 0.3$, $\Omega_\Lambda = 0.7$; $\sigma_8 = 0.9$ the dot–dashed line), and one in which the energy density is divided evenly between $\Omega_{\rm m}$ and Ω_Λ (Cosmo-5; long dashed line).

In general, the higher the matter density, the higher the merger fraction within the halo merger models. This is parametrized in Section 5.2 in terms of the value of Ω_Λ. The halo merger fraction begins to turn over when there is a higher Λ term in the cosmology. This is as expected, given that detailed numerical models of galaxy formation have shown for many years that the large-scale structure of the universe depends strongly upon the assumed cosmology, as well as the temperature of the dark matter particle (e.g. Jenkins et al. 1998; Menci, Fiore & Lamastra 2012).

We later examine in Section 5 how the halo merger history relates to the galaxy merger history, and how comparisons between the two can potentially reveal information concerning cosmological parameters, as well as information regarding the measured galaxy merger history.

We parametrize the halo merger evolution for different cosmologies using the same power-law formalism explained in Section 3.1. These resulting fits are listed in Table 2 along with their name and associated cosmological parameters. Just as for galaxies of different halo masses, we find that the values of f_0 do not vary significantly between the different cosmologies, and that the most variation is within the values of m. In general, we find that the higher the value of Ω_Λ, the higher the fitted value of the power-law slope, m. The

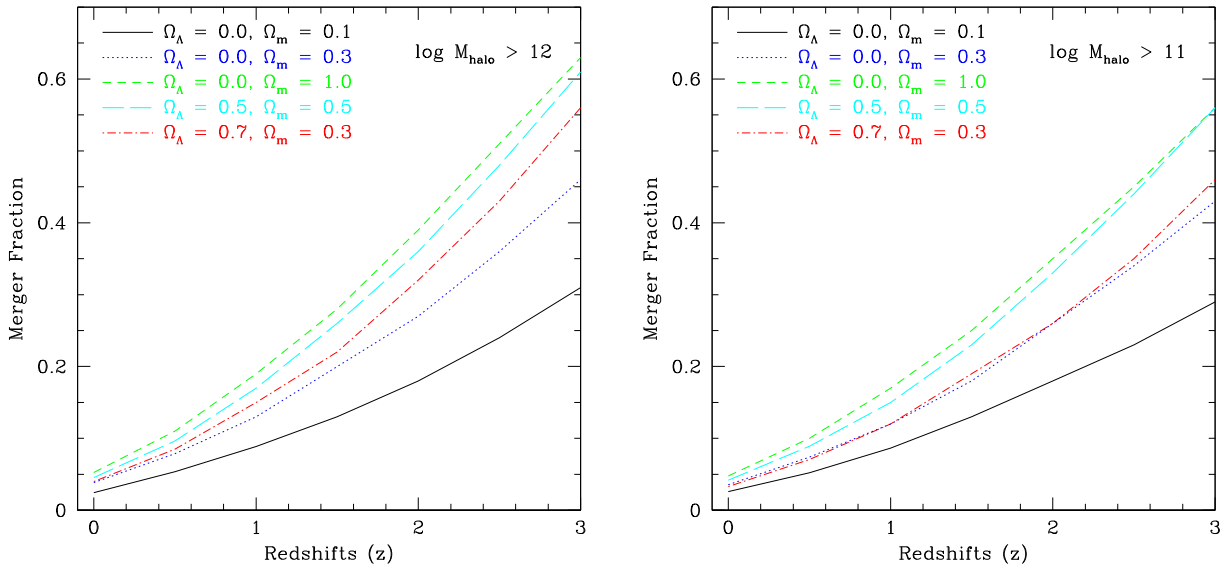

Figure 2. The halo merger histories for (a) haloes with masses $M_{\rm halo} > 10^{12}$ $M_\odot$ and (b) haloes with masses $M_{\rm halo} > 10^{11}$ $M_\odot$. The various lines show how the merger history varies with redshifts for haloes of these given masses and using the cosmologies shown in the upper left. In general, we find that cosmologies with the highest matter densities have the highest merger fractions, although higher values of Λ produce a smaller merger fraction at a given redshift.

Table 2. The cosmological models we use in this paper to compare with the observed merger fractions and their various fitted parameters. These are for galaxies with halo masses of $M_{\rm halo} > 10^{12}$ $M_\odot$. Listed are each model's Ω_Λ, $\Omega_{\rm m}$ and σ_8 values. We also show the best-fitting f_0 and m values for the power-law fits as discussed in Section 3.1.

Model	Ω_Λ	$\Omega_{\rm m}$	$\Omega_{\rm tot}$	σ_8	f_0	m
Cosmo-1	0.0	0.1	0.1	0.9	0.027	1.73
Cosmo-2	0.7	0.3	1.0	0.9	0.032	1.92
Cosmo-3	0.0	0.3	0.3	0.9	0.035	1.82
Cosmo-4	0.0	1.0	1.0	0.9	0.052	1.73
Cosmo-5	0.5	0.5	1.0	0.9	0.041	1.88
Cosmo-6	0.7	0.3	1.0	0.7	0.038	1.93
Cosmo-7	0.7	0.3	1.0	0.8	0.034	1.97
Cosmo-8	0.7	0.3	1.0	1.0	0.032	1.94
Cosmo-9	0.7	0.3	1.0	1.1	0.033	1.88

average m value for $\Omega_\Lambda = 0.7$ is $m = 1.93$, while for $\Omega_\Lambda = 0.3$ it is $m = 1.76$. The decline in mergers is therefore steeper for higher values of Λ due to the accelerated expansion, lowering the number of mergers at a faster rate.

3.3 Halo merger dependence on σ_8

One cosmological parameter that can vary, and depends on large-scale structure, and therefore also the halo and galaxy formation history, is the value of σ_8, the normalization of the matter power spectrum, as measured in the rms dispersion of total mass density within 8 Mpc spheres.

We show the variation of the halo merger histories using the standard cosmology of $\Omega_{\rm m} = 0.3$, $\Omega_\Lambda = 0.7$ but with different variations of the value of σ_8 in Fig. 3. The differences in the predicted halo merger history between these values of σ_8 are smallest at $z < 1$, where the merger fraction only varies by $\delta f_{\rm halo} \sim 0.02$ over the range of $\sigma_8 = 0.7$ to 1.1. For the $\sigma_8 = 0.7$ models, we find at $z = 1$ that the halo merger fraction is $f_{\rm halo} = 0.15$, while for $\sigma_8 = 1.1$

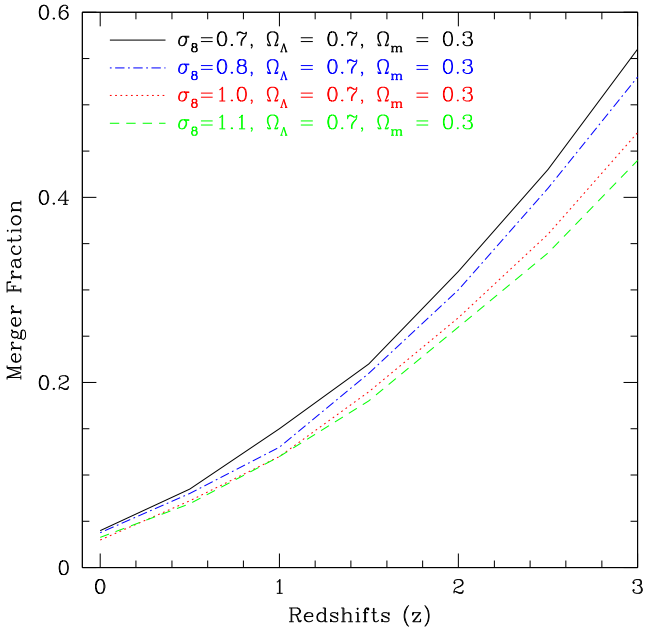

Figure 3. The evolution of the halo merger fraction for haloes with $M_{\rm halo} > 10^{12}$ $M_\odot$ as a function of the value of σ_8. The range we show here is for $\sigma_8 = 0.7$–1.1, with the highest halo merger fractions for those evolving within a universe that has the lowest σ_8.

the halo merger fraction is $f_{\rm halo} = 0.12$. This implies that at a given redshift the accuracy of our merger fractions would have to be better than a few percentage, which is easier to accomplish than that required to distinguish between various values of likely different Ω cosmologies (Section 5).

We tabulate in Table 2 the values of the best-fitting power-laws to these merger histories at various values of σ_8. We find a strong linear relationship between the halo merger fraction and the value of σ_8, such that,

$$f_{\rm halo} = (-0.230 \pm 0.06) \times \sigma_8 + (0.592 \pm 0.006), \quad (11)$$

at a redshift of $z = 2.5$. This demonstrates that there are higher values of both f_0 and m for universes with higher values of σ_8. This implies that when the rms fluctuations of spheres of dark matter with a radius of 8 h^{-1} Mpc are smaller, there is a higher rate of merging within the universe. This result is likely due to the fact that the value of σ_8 is directly tied to the halo mass function. That is, when σ_8 increases this effectively shifts the halo mass function to higher values. This then increases the normalization needed to reach the same vale of the merger rate as at a lower value of σ_8. From Table 1, we can see that lower mass haloes have a lower merger rate and thus a higher σ_8 pushes the effective scaling lower, thus creating a lower merger rate at a given halo mass.

4 COMPARISON OF OBSERVED GALAXY MERGERS TO SIMULATED GALAXY MERGERS

In this section, we discuss the comparison of our observations of the galaxy merger history with the theoretically simulated galaxy merger histories. We do this before we examine the comparison of halo merger histories to galaxies, as comparing with simulated galaxy mergers is a more direct comparison, although it largely fails as we show.

4.1 Background

While the galaxy merger history as predicted in various simulations has been discussed in detail elsewhere (e.g. Bertone & Conselice 2009; Jogee et al. 2009; Hopkins et al. 2010), we give a short summary here, as well as a comparison to the halo models. We show on Fig. 1 as the solid dark line towards the lower part of the plot the galaxy merger history for systems selected by a stellar mass limit of log $M_* > 10$ as predicted in the Millennium simulation. This roughly corresponds to a halo mass a factor of 10 higher, based on the results from Twite et al. (in preparation) who investigate the ratios of stellar and halo masses for galaxies (see Section 5.1). In general, it appears that the predicted galaxy merger history is much lower than the halo merger history at roughly the same selection. The ratio between the halo and galaxy merger fractions from the Millennium simulation is roughly constant, at a ratio of $\sim$7.5 up to redshifts of $z \sim 3$.

We directly compare the predicted galaxy merger history from the Millennium simulation to merger fraction data in Figs 4 and 5. The first piece of evidence to take away from this figure is that the predicted galaxy merger histories are quite different from the observed galaxy merger histories. In fact, as discussed in e.g. Jogee et al. (2009) and Bertone & Conselice (2009) the merger histories for galaxies does not match the observations, with too few major merger observed than what is predicted in the galaxy merger histories from the Millennium simulation (Figs 4 and 5), although in Section 4.3 we discuss how this changes when using WDM galaxy merger simulations.

An important issue is that the galaxy merger history can, and does, depend strongly on the galaxy formation model used. We show this in detail in Fig. 4 where four different realizations of the Millennium simulation are shown from Bertone, De Lucia & Thomas (2007), Bower et al. (2006), De Lucia et al. (2006) and Guo et al. (2011). As can be seen, these models do not agree with the observations. It is interesting as well that the predicted galaxy mergers within different realizations of the Millennium simulation tend to agree with each other for $M_* > 10^{10}$ M$_\odot$ galaxies, but widely disagree for those with masses in the $M_* > 10^{11}$ M$_\odot$ range. The reason for this is due to these models not agreeing on which galaxies belong in which halo, which becomes more of an important issue at higher halo masses. These massive galaxies are on the exponential tail of the mass function and therefore any differences in the star formation history or feedback can produce significant differences in the merger history through matching which galaxy is in which halo (see also Bertone & Conselice 2009).

4.2 Detailed comparison of models with data

With one exception, the observed galaxy merger histories with redshift start at low values, peak at redshifts of around $z \sim 2$, and then decline thereafter at higher redshifts. This is similar to what is found within the Millennium simulation predictions for galaxies, although often at a lower level. In contrast, the merger history for haloes continues to steeply increase at higher redshifts at all masses (Fig. 1).

This difference is very likely due to the way sub-haloes are dealt with within the Millennium simulation. When a galaxy is accreted into a larger halo it loses all of its cold gas, and therefore cannot produce new stars, and thus when the merger occurs after some dynamical friction time-scale, the mass ratio of the merger is low. These mergers thereby end up as minor mergers, although in some ways in baryons these would still be major mergers if the striped gas was included. In fact, the high minor-merger fraction predicted in the Millennium simulation suggests that this might be occurring (Bertone & Conselice 2009). Furthermore, simple computational differences, such as using different methods to calculate the feedback from supernova, can dramatically change the measured galaxy merger history (Bertone & Conselice 2009). Investigating in more detail these differences is important, but we do not discuss this issue further in this paper.

To compare these different observed merger histories, for haloes and galaxies and the actual merger histories, in a more quantitative way, we characterize the merger histories by fitting the predicted galaxy merger histories with the power-law form given by equation (9). The results of these fits are shown in Table 3 . Fits such as these typically only provide a good fit to the data up to some redshift where the merger fraction begins to turn over to lower values. However, with some exceptions, these are good fits to the data at $z < 3$ for both halo models, and the actual observed galaxy mergers.

When we fit these merger fractions to the halo merger histories, we find that their power-law indices are all $m \sim 2$. This differs from what we find when we compute the same power-law indices for observed galaxies, with numbers ranging from $m = 3$ to $m = 1$ (Tables 1–3; e.g. Conselice et al. 2009; Lotz et al. 2011). Galaxy mergers selected in the manner we use for the halo mergers generally always find that $m \sim 3$ (e.g. Conselice et al. 2008; Bluck et al. 2012). We also list in Table 3 the fitted power-law parameters for both CDM and WDM simulations which we discuss in Section 4.

Overall, we find that the halo merger history is significantly different from what is predicted in galaxy merger evolution from the Millennium simulation. In fact, the halo merger history is a better description of the observed galaxy merger history than the predicted galaxy mergers using the same simulations (Section 5). This however shows that the fundamental merger histories for galaxies and haloes can be quite different, and new approaches of establishing the connection between halo and galaxy mergers is needed.

While there is not a good match between semi-analytical model predictions of galaxy mergers and the observations, when deriving the merger history through abundance matching (e.g. Hopkins

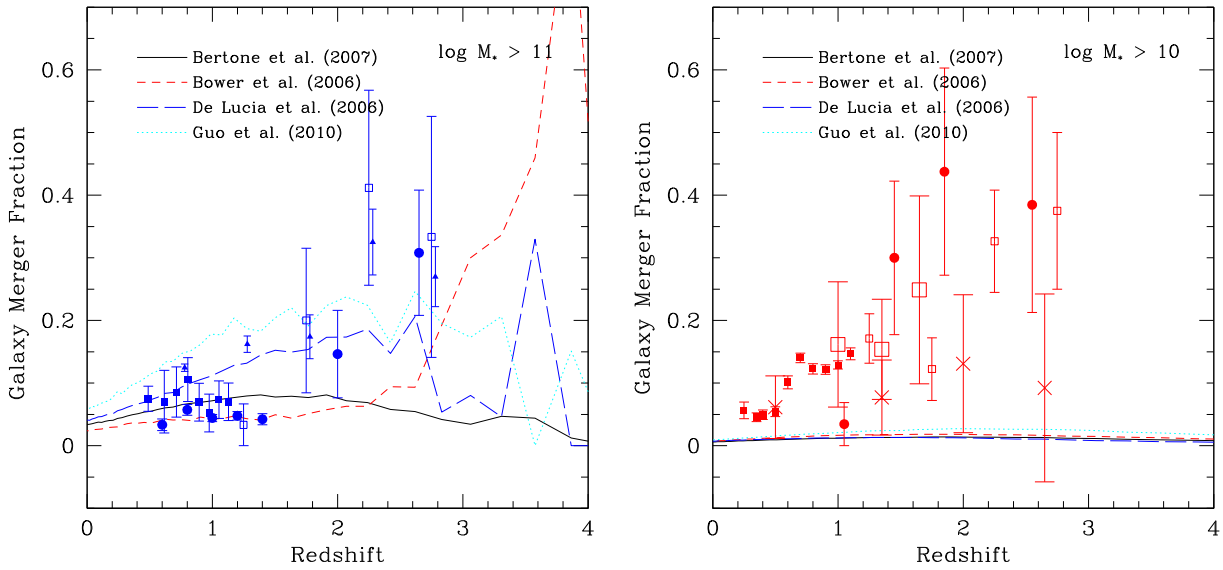

Figure 4. The predicted merger history for galaxies using different realizations of the semi-analytical Millennium I simulation. Shown here are models from Bertone et al. (2007, solid line), Bower et al. (2006, dashed red line), De Lucia et al. (2006, long-dashed blue line) and Guo et al. (2011, cyan dotted line). The large variation in models seen for the $M_* > 10^{11}$ $M_\odot$ galaxies is solely due to the identification of galaxies with haloes, as the underlying merger history for the haloes in these simulations are identical. The points with error bars shown are actual measures of the merger fraction for galaxies as a function of redshift. The blue points on the left show the merger history for $M_* > 10^{11}$ $M_\odot$ systems including results from Conselice et al. (2009, solid boxes at $z < 1.2$); Bluck et al. (2009, 2012, solid circles at $z > 0.5$ and solid triangles) and Mortlock et al. (2013, open boxes at $z > 1$). The red points on the right are for $M_* > 10^{10}$ $M_\odot$ galaxies, including results from Conselice et al. (2003) at $z > 1$ in the HDF (solid circles); Conselice et al. (2009, solid boxes at $z < 1.2$); and Mortlock et al. (2013, small open boxes at $z > 1$). Also shown are pair merger fractions at separations of <30 kpc: Man et al. (2012, crosses at $z > 1$); Lopez-Sanjuan et al. (2010, large open boxes). These points are used in later figures as well.

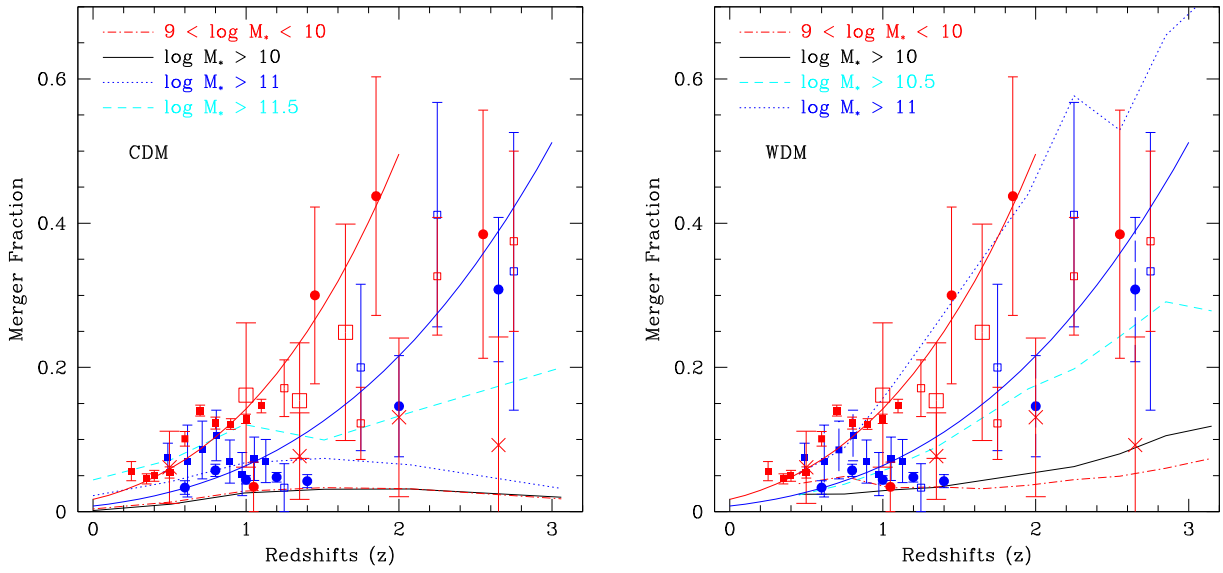

Figure 5. The merger history for galaxies using two simulations utilizing different dark matter particle temperatures out to $z = 3$. The left-hand panel shows the semi-analytical merger history predictions for galaxies with various stellar masses as taken from the Millennium simulation results of Bertone et al. (2007). The various lines show the merger fraction, as measured using the same criteria as used to select the merger histories for the haloes shown in in Fig. 2. The right-hand panel shows the merger history at the same stellar mass limits but with using a simulation with WDM (Menci et al. 2012). The solid red line is the best-fitting power law to the observed evolution in galaxy mergers for the $M_* > 10^{10}$ $M_\odot$ galaxies, while the solid blue line shows the corresponding best fit for the $M_* > 10^{11}$ $M_\odot$ galaxies. The data points used for comparison are the same as in Fig. 4.

et al. 2010), there is a better match with data compared with theory results and simulations at some halo mass ranges (see also Figs 4 and 5). We show this comparison for abundance matched mergers in Fig. 6 where the galaxy merger data is plotted alongside corresponding mergers derived from abundance matched samples from Hopkins et al. (2010) as measured using the *WMAP*1, *WMAP*3 and *WMAP*5 cosmological parameters. These cosmological parameters are (Ω_m, Ω_Λ, h, σ_8, n_s) = (0.3, 0.7, 0.7, 0.9, 1.0) for the

Table 3. The best-fit power-law parameters in the form $f_m = f_0 \times (1+z)^m$ based on the output from the galaxy merger simulations based on the Millennium simulation and the WDM simulations of Menci et al. (2012).

Mass ranges	Dark matter	f_0	m
$9 < \log M_* < 10$	CDM	0.007 ± 0.002	1.77 ± 0.43
$\log M_* > 10$	CDM	0.005 ± 0.002	2.00 ± 0.56
$\log M_* > 11$	CDM	0.030 ± 0.004	1.19 ± 0.21
$\log M_* > 11.5$	CDM	0.050 ± 0.010	0.99 ± 0.14
$9 < \log M_* < 10$	WDM	0.010 ± 0.002	1.40 ± 0.21
$\log M_* > 10$	WDM	0.006 ± 0.001	2.07 ± 0.13
$\log M_* > 10.5$	WDM	0.017 ± 0.003	2.04 ± 0.14
$\log M_* > 11$	WDM	0.040 ± 0.010	1.89 ± 0.15

Table 4. The best-fitting power-law parameters in the form $f_m = f_0 \times (1+z)^m$ based on fits to dark halo mergers with different values of ω. These fits are for haloes with $M_{halo} > 10^{11}$ M$_\odot$.

ω	f_0	m
-0.33	0.0380 ± 0.0001	1.634 ± 0.003
-0.40	0.0374 ± 0.0002	1.661 ± 0.004
-0.50	0.0360 ± 0.0003	1.705 ± 0.007
-0.60	0.0344 ± 0.0003	1.749 ± 0.007
-0.70	0.0331 ± 0.0003	1.791 ± 0.007
-0.80	0.0320 ± 0.0002	1.826 ± 0.005
-0.90	0.0312 ± 0.0001	1.855 ± 0.004
-1.00	0.0307 ± 0.0001	1.878 ± 0.002
-1.10	0.0304 ± 0.0001	1.895 ± 0.002
-1.20	0.0302 ± 0.0001	1.908 ± 0.004

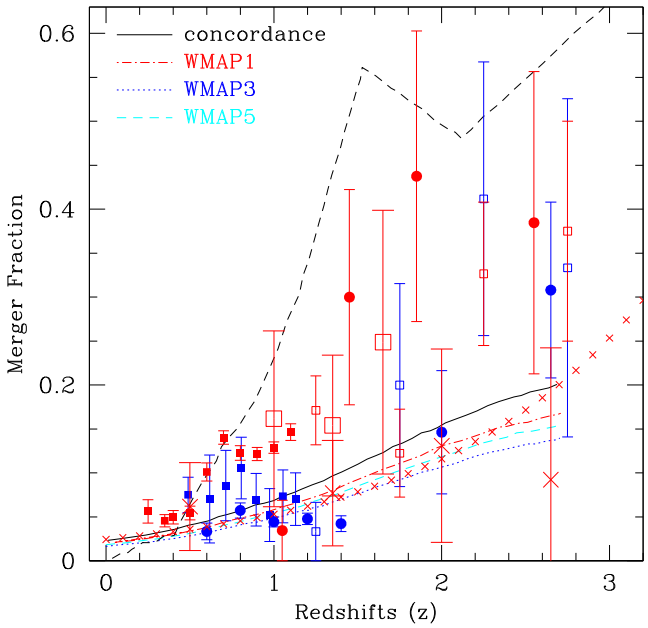

Figure 6. Plot of the observed and predicted galaxy merger history. The predicted lines are from the *WMAP*1, *WMAP*3 and *WMAP*5 cosmologies used to calculated the merger history in Hopkins et al. (2010). The data with error bars are the same as used in Fig. 4. The dashed line at the upper end of the figure is from numerical models by Maller et al. (2006) and the red dotted crosses are from Stewart et al. (2009).

concordance cosmology, (Ω_m, Ω_Λ, h, σ_8, n_s) = (0.27, 0.73, 0.71, 0.84, 0.96) for *WMAP*1, (Ω_m, Ω_Λ, h, σ_8 and n_s) = (0.268, 0.732, 0.704, 0.84, 0.96) for *WMAP*3, (Ω_m, Ω_Λ, h, σ_8, n_s) = (0.274, 0.726, 0.705, 0.776, 0.95) for *WMAP*5.

The different lines in Fig. 6 show the different cosmologies used to measure the merger history. This is slightly different from our approach, which is to see how the merger history varies as a function of cosmology, as opposed to determining how the merger history changes due to different measured cosmological parameters.

As can be seen, even within these models there is a slight difference in the calculated merger history from abundance matching. The merger histories here are still lower than what we find observationally; however, the highest merger fractions are for the cosmologies with the highest value of Ω_m. As the recent *Planck* cosmology has an even higher Ω_m than the concordance model (Planck Collaboration; Ade et al. 2013), the merger history using this cosmology would be higher than those shown here, and would better match the data.

The important take away message here is that the halo merger history does a much better job of matching the observed galaxy merger history than any galaxy merger history prediction. This is a fundamental insight and one in which we now expand on in Section 5, with the use of the halo merger models as a measure of cosmology. The idea we explore in this paper is to not use the predicted galaxy formation merger histories, but the halo merger histories and to do 'inverse modelling' whereby the galaxy sample's halo mass is derived, and then compared with halo mass merger histories. This side-steps the need for understanding the detailed physics in simulations of galaxy formation, but does require knowledge of how to convert from observed galaxy to inferred halo mass. This is essentially what is done when using galaxy cluster as observational probes – the cluster's dark matter is measured and compared with theory, especially for cosmological tools such as galaxy cluster number density (e.g. Vikhlinin et al. 2009).

4.3 Variation with dark matter particle temperature

We also investigate how the galaxy merger history varies as a function of the temperature of the dark matter particle. This is a different topic in some ways from the variation in structure formation depending on cosmological parameters, yet this is another cosmological feature that does influence structure, and thus we include it here. Since the structure formation models we examined before all depend on CDM, we utilize the Menci et al. (2012) dark matter semi-analytical models to make the comparison with the CDM models from the Millennium simulation. In Fig. 5, we show the merger history for the CDM based Millennium simulation as well as a WDM simulation from Menci et al. (2012).

Fig. 5 shows that the WDM simulations do a better job of matching the observations, which is also seen in comparisons to observed galaxy number densities in the CDM and WDM simulations (e.g. Menci et al. 2012). Effectively, the merger fraction in WDM galaxy simulations is a factor of 1.3 higher for systems with $M_* > 10^{10}$ M$_\odot$, and a factor of 3 higher at masses of $M_* > 10^{11.5}$ M$_\odot$. It is clearly the more massive systems (Fig. 5) which show the greatest difference between the CDM and WDM predictions. As CDM halo mergers, as well as those predicted in the Millennium simulation itself, predict a higher halo merger rate similar to the observed galaxy rate, then it is likely that the problem with the CDM galaxy mergers is not due to CDM itself, but due to how baryons are handled in these simulations.

5 OBSERVATIONS OF MERGERS AS A COSMOLOGICAL TOOL

The previous section showed that observed galaxy mergers have a different evolution than that seen in predictions of galaxy mergers. In this section, we discuss in detail how to compare simulated halo mergers with observed galaxy mergers. This is a non-trivial comparison to make, and depends on several assumptions that we discuss in detail. One of these issues is the correspondence between the halo and stellar masses which is required to match halo histories to that of galaxies, or on just a practical level matching a halo mass to a stellar mass. The relationship between these two masses is ideally well defined and has a small scatter to minimize mismatches between the haloes and galaxies. Other issues in a comparison to haloes and galaxies have to do with relating the time-scales for halo merging to those of galaxy mergers.

We previously discussed briefly how there is better agreement between predicted halo mergers and the observed galaxy merger fractions. One of our major conclusions is that it is better to compare the observed galaxy merger history with these predicted halo mergers rather than with the predicted galaxy mergers. In this section, we present a new method for comparing the observed merger history to the predicted halo merger history as a measurement of cosmology. We show that this can be done through several steps, each containing a certain amount of uncertainty. This process is such that we convert the observed stellar mass selected sample into a halo mass using relations that we discuss based on halo abundance matching and kinematic data (Section 5.1). These relations are discussed in more detail in Twite et al. (in preparation). There are uncertainties in these conversions which we discuss and include in our analysis. the first part of this process is the conversion or matching of halo and stellar masses to effectively use the halo mass mergers we discussed in Sections 2 and 3. We conclude this section with how to best compare the modelled dark matter halo mergers to the observed galaxy mergers, especially in the future when better data and simulations are available.

5.1 Relation between halo and stellar mass

A major issue that needs to be addressed in any paper that compares halo properties to galaxies is how to relate the stellar mass of a galaxy to its underlying halo mass. This relates back to our idea of comparing with CDM, and other dark matter based models. What we therefore need is an accurate way to relate the observed stellar mass to the inferred halo/total masses of galaxies.

This can be done in a number of ways, including kinematics and gravitational lensing to derive the total masses of galaxies. This problem has been investigated at high redshift in several studies, including Conselice, Blackburne & Papovich (2005), Foucaud et al. (2010) and Twite et al. (in preparation). All of these studies conclude that the dark matter to stellar matter ratio evolves together such that the different components of the assembly history are increasing at a similar rate. This is an important aspect, as it allows us to compare the observed merger history of galaxies which is based on a stellar mass selection, to that of halo selection, which is predicted in models. Yet another approach towards understanding the relationship between stellar and halo masses is halo abundance matching (e.g. Conroy & Wechsler 2009; Twite et al., in preparation) which we also investigate for relating stellar and halo masses.

We calculate the abundance matching derived relation between stellar and halo masses using the stellar mass functions from Mortlock et al. (2011). We match number densities from galaxies with measured stellar masses to dark matter halo abundances at the same redshifts. This allows us to associate each stellar mass range with a halo mass range. This is described in more detail in Twite et al. (in preparation).

In summary, to compute this relation the mass function of dark matter haloes (including sub-haloes) is assumed to be monotonically related to the observed stellar mass function of galaxies with zero scatter. This relation is given by

$$n_{\rm g}(>M_{\rm star}) = n_{\rm h}(>M_{\rm halo}) \tag{12}$$

where, the values $n_{\rm g}$ and $n_{\rm h}$ are the number density of galaxies and dark matter haloes, respectively.

We derive these values for the haloes from the Jenkins et al. (2001) modification to the Sheth & Tormen (1999) halo mass function using the analytic halo model of Seljak (2000). We also generate the linear power spectrum using the fitting formulae of Eisenstein & Hu (1999), the same one we use to predict the halo mergers. The predicted number density of dark matter haloes is then given by

$$n_{\rm h}(>M_{\rm halo}) = \bar{\rho} \int_{M_{\rm min}}^{\rm inf} \frac{\langle N \rangle}{M_{\rm halo}} f(\nu)\, {\rm d}\nu, \tag{13}$$

where $f(\nu)$ is the scale-independent halo mass function, $\nu = [\delta_c/\sigma(M_{\rm halo})]^2$ ($\delta_c = 1.68$ is the value for spherical overdensity collapse). $\sigma(M_{\rm halo})$ is the variance in spheres of matter in the linear power spectrum, $\bar{\rho}$ is the mean density of the Universe and $\langle N \rangle$ is the average number of haloes, including sub-haloes where we assume the fraction of sub-haloes ($f_{\rm sub}$) is described by

$$f_{\rm sub} = 0.2 - \frac{0.1}{3} z, \tag{14}$$

as in Conroy & Wechsler (2009). This method of halo abundance matching does a good job at matching observations at multiple epochs (e.g. mass-to-light ratios, clustering measurements).

The halo abundance matching we use for our main ΛCDM cosmology include errors that incorporate the difference in the abundance matching at the redshift bounds of each bin, and the uncertainty due errors in the stellar mass functions. We investigate the same abundances using the mass function and galaxy bias as that of Tinker et al. (2008) and Tinker et al. (2010). These results are very close to that of the Jenkins et al. (2001) halo mass function, and its resulting bias. We also find that the halo to stellar mass relationship from abundance matching, using our main ΛCDM cosmology, and the cosmology used in Conroy & Wechsler (2009) extracted using DEXTER are almost identical at higher redshifts. Our results also match the redshift $z = 1$ Conroy & Wechsler (2009) work well considering our redshift bin is slightly higher, and we use different galaxy stellar mass functions. Similarly to Conroy & Wechsler (2009) who do not trust their $z > 1$ results, we do not place much emphasis on our high-z results below the relevant stellar mass limits. e.g. for $z = 2$ at $\log M_* > 10^{10.5}$ $M_\odot$. The evolution in shape at the high-mass end is also in agreement with Conroy & Wechsler (2009). Therefore, the range of merger histories for different cosmologies in the abundance matching will not vary by much.

Although this paper is not focused on abundance matching, which will be described in more detail in Twite et al. (in preparation), another issue that we investigate is how well our abundance matching can reproduce the angular correlation function of galaxies to check for halo bias within our halo abundance matching models. It should be noted that this is intended as a rough check and not a robust fit of the galaxy HOD as this is not the focus of this work. We produce angular correlation functions using our HOD code with a simplified version of the five-parameter HOD model (e.g. Zheng

et al. 2005), where $N_{\rm centrals} = 1$ if $M_{\rm h} > M_{\rm h}$ ($M_*^{\rm min}$) and $M_{\rm h} < M_{\rm h}$ ($M_*^{\rm max}$), and $N_{\rm sat} = [(M - M_0)/M_{1'}]^{\alpha}$. Here, we have set $\alpha = 1$, $\log_{10}(M_0) = \log_{10}(M) - 1.5$ and $\log_{10}(M_{1'}) = \log_{10}(M) + 1.0$, which correspond to average HOD fit parameters (e.g. Zehavi et al. 2011).

We also compare the resulting correlation function with the power-law fits from Foucaud et al. (2010). Here, we have assumed a Gaussian redshift distribution (whereby the Gaussian was centred on the middle of the redshift bin and had $\sigma =$ (bin-width/2)/3, and we then use the Limber (1954) equation to transform to the angular correlation function. We follow the formalism of the Tinker et al. (2005) $n_{\rm g}$ matched method to obtain the galaxy correlation function. We find that our large-scale clustering is in good agreement with the power law for the $z = 1$ samples; however, it is likely that the power law should be steeper for such massive galaxies at high redshift, and the small-scale clustering is at about the right amplitude. We can therefore confidently say that the abundance matching reproduces the ball park correlation functions for galaxies, at a similar level to what is stated in Conroy & Wechsler (2009).

We show the comparison between halo masses derived in this way and the stellar masses at the same limit in Fig. 7 from redshifts from $z = 1$ to $z = 3$ using two different methods. There is clearly little evolution in the halo to stellar mass ratio as a function of redshifts within our masses of interest, which is also what we find when we investigate this relationship using the observable relations from internal motions. Fig. 7 shows the relationship between the stellar and halo masses for galaxies up to $z = 3$ calculated in two different ways.

There is some disagreement at the lower mass range; however, this is due to the fact that there is unlikely a 1:1 galaxy–halo ratio at these masses. Hence, we get an overestimate of the halo masses for these systems. This is expected to some degree within this formalism, and this effect has been seen before by e.g. Conroy & Wechsler (2009). Note that we only use Fig. 7 in the stellar mass range where our galaxies are found (log $M_* = 10$–11.5), and do not consider these relations valid at high masses where the halo occupation is very large and where this relation breaks down.

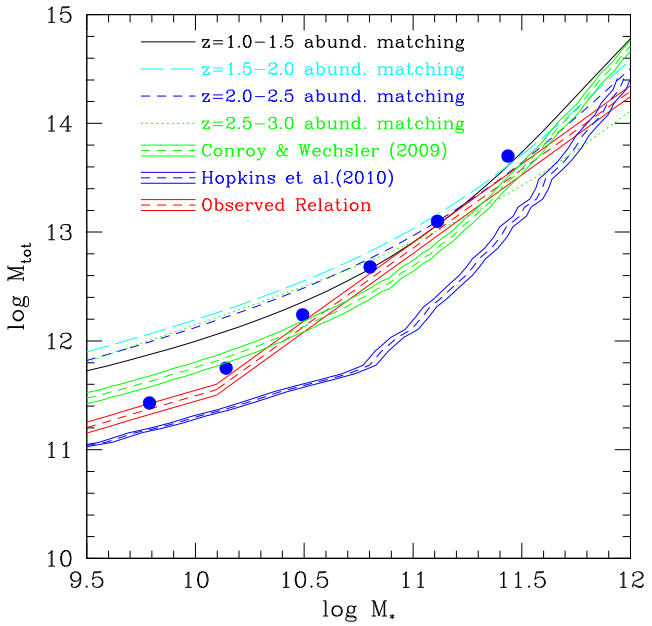

Figure 7. The relationship between the stellar mass and halo mass. The solid blue round points and red long-dashed hatched lines show the stellar mass vs. halo mass relation derived through two slightly different methods using kinematics of $z < 1.4$ galaxies (Twite et al., in preparation). The other lines are from our halo abundance matching fitting, while the dashed line with two solid lines around it are from abundance matching from Hopkins et al. (2010) and Conroy & Wechsler (2009).

Shown in Fig. 7 is the kinematic relation found by Twite et al. (in preparation) between the stellar masses of galaxies and their total masses as measured through kinematics. The relation between these is given by

$$\log(M_{\rm tot}) = (\alpha)\ \log(M_*) + (\beta), \quad (15)$$

where the values of α and β are a function of the stellar mass. We calculate (see also Twite et al., in preparation) that for log $M_* < 9.9$, $\alpha = 0.58 \pm 0.03$, $\beta = 5.56 \pm 0.27$, while for systems with log $M_* > 9.9$, $\alpha = 1.44 \pm 0.06$ and $\beta = -3.11 \pm 0.61$. In Fig. 7, we plot this relation alongside the relation for the abundance matching. In general, there is a correlation such that $M_{\rm halo}/M_* \sim 10$, with a relatively small scatter.

This implies that we are able to match the halo mass to our measured stellar masses for our galaxies in which we measure the stellar masses and merger histories from up to $z = 3$. When we do these comparisons we find that the log $M_* = 10$ limit corresponds to log $M_{\rm halo} = 11.3$ and log $M_* = 11$ (see Section 5.2) corresponds to log $M_{\rm halo} = 12.7$. We therefore use these limits for matching our observational data on mergers in galaxies to those in haloes. Since we only use these two limits of stellar mass, we are almost always certain that these systems dominate their respective haloes.

5.2 Comparing halo mergers with observed galaxy mergers

With the caveats explained above, and using the halo mass to stellar mass comparisons in Section 5.1 we can now compare the halo merger histories to the observed galaxy merger fractions.

5.2.1 Applying the stellar mass to halo mass relation

The key to performing the comparison between the observed mergers and the predicted halo mergers is using the $M_{\rm halo}$ versus M_* relation described in Section 5.1 to match the halo mass with the stellar mass from our observations. This must be done carefully in two different ways. The first is that we must convert the observed stellar mass of each galaxy to a halo mass. However, we also must be sure that the mass ratios used in the predicted halo mergers, in which we use the value of >1: 4, is the same as the mass ratio used in the selection of the observed mergers. The issue is that if we use a >1:4 stellar mass ratio selection to find mergers, using the relation from equation (15) this gives us a corresponding total mass ratio of ∼ 1:8. Likewise, a halo mass ratio of 1:4 gives us a stellar mass ratio of ∼ 1:2.6. Therefore, we have to ensure that any comparisons between the halo merger fraction evolution, and the galaxy merger fraction are done with the same underlying mass ratios.

For the mergers found through their high asymmetries, the merger ratio for galaxies in total mass is >1:4 based on simulations using dark matter (Conselice 2006) as well as through combined dark matter + baryon simulations (Lotz et al. 2010a). However, this is not the case for the galaxies in pairs. To address this, we investigate the merger fractions for galaxies which correspond to total mass mergers of >1:4. This corresponds to a stellar mass ratio of >1:2.6 using equation (15). We therefore calculate the stellar mass merger ratios using values of >1:2.6. These merger fractions with this ratio are therefore used on all the plots within this paper. We determine the

merger fraction at this stellar mass ration by using the observations from Bluck et al. (2012). We use this to correct other pair fractions from Man et al. (2012) and Lopez-Sanjuan et al. (2010), with the assumption that the relative fractions change in the same way as in the Bluck et al. (2012) study. Regardless, the vast majority of our comparisons are done using the CAS mergers where the total mass ratios are already >1:4.

5.2.2 *Comparison of observed and predicted mergers*

Using the information above, we show in Fig. 8 a direct comparison between the halo merger history predictions which we have discussed throughout this paper, and the observed galaxy merger histories based on our stellar mass selection. Fig. 8 shows that there is general agreement between the shape and normalization of the merger history for the predicted haloes and the observed galaxy merger histories. To make a quantitative comparison, we use the conversion factors from equation (15), with its associated uncertainties to determine the halo mass for the corresponding selection of stellar mass. For log $M_* > 10$, this corresponds to a selection of log $M_{\rm halo} = 11.3 \pm 0.4$. We then use the relations discussed in Section 3.1 to determine the merger fraction for galaxies at this halo mass and their associated uncertainties as a function of redshift. As discussed in Section 3.1, there is very little variation in the merger fraction for haloes of different masses at a given redshift. For example, at $z \sim 2.5$, the merger fraction with an uncertainty given by the models and conversion uncertainty is $f_{\rm halo} = 0.35^{+0.01}_{-0.02}$.

Our relatively large observational errors on the merger fraction evolution cannot easily distinguish between these various models currently, an issue we discuss in more detail below in terms of future surveys that can improve this comparison with data. We however carry out a full analysis of the best-fitting model using a reduced χ^2 approach, and using the uncertainties calculated using the methods described above across all redshifts. We do this by matching the model with the corresponding halo mass to our stellar mass derived galaxy merger measurements. We then utilize the best-fitting power laws to determine the χ^2 of each fit. The reduced χ^2 values range from 4.8 to 14.43, with the best-fitting model the concordance cosmology with $\Omega_\Lambda = 0.7$ and $\Omega_{\rm m} = 0.3$. The data also rule out that the universe has a low matter density of $\Omega_{\rm m} = 0.1$, although in terms of the comparison there is a similarity between the merger history for models with $\Omega_{\rm m} = 0.3$, $\Omega_\Lambda = 0.7$ and $\Omega_{\rm m} = 0.3$, $\Omega_\Lambda = 0$.

We furthermore show in Fig. 9 the variation of the halo merger fraction as a function of Ω_Λ at $z = 2.5$ with the assumption that $\Omega_\Lambda + \Omega_{\rm m} = 1$ holds throughout. The best-fit relation between the merger fraction and the value of Ω_Λ is given by

$$f_{\rm halo} = \alpha \times \Omega_\Lambda + \beta = \alpha \times (1 - \Omega_{\rm m}) + \beta, \quad (16)$$

where the values for the fit for $\Omega_\Lambda < 0.55$ are $\alpha = -0.05 \pm 0.01$ and $\beta = 0.41 \pm 0.01$. For $\Omega_\Lambda > 0.55$, the best fit is given by $\alpha = -0.24 \pm 0.02$ and $\beta = 0.52 \pm 0.01$. The relation between the halo merger values and Ω_Λ is such that at $\Omega_\Lambda < 0.55$ there is very little variation between the value of Ω_Λ and the merger fraction. This relation becomes steeper for values $\Omega_\Lambda > 0.6$, making it a more sensitive measurement of Ω_Λ and $\Omega_{\rm m}$.

Using our best measured merger fraction of $f_{\rm m} = 0.31 \pm 0.07$ at $z = 2.5$, we find that this formally leads to a measured $\Omega_\Lambda = 0.84^{+0.16}_{-0.17}$, which is very uncertain compared to other leading methods of finding Ω_Λ, but still demonstrates consistency with previous work, and that there is at least broad agreement between cosmology and galaxy formation as seen through mergers. The error bars on this measurement come from the uncertainty in the theoretical fit and the uncertainty in the measured merger fraction from Mortlock et al. (2013) based on CANDELS data and incorporating stellar mass and redshift uncertainties.

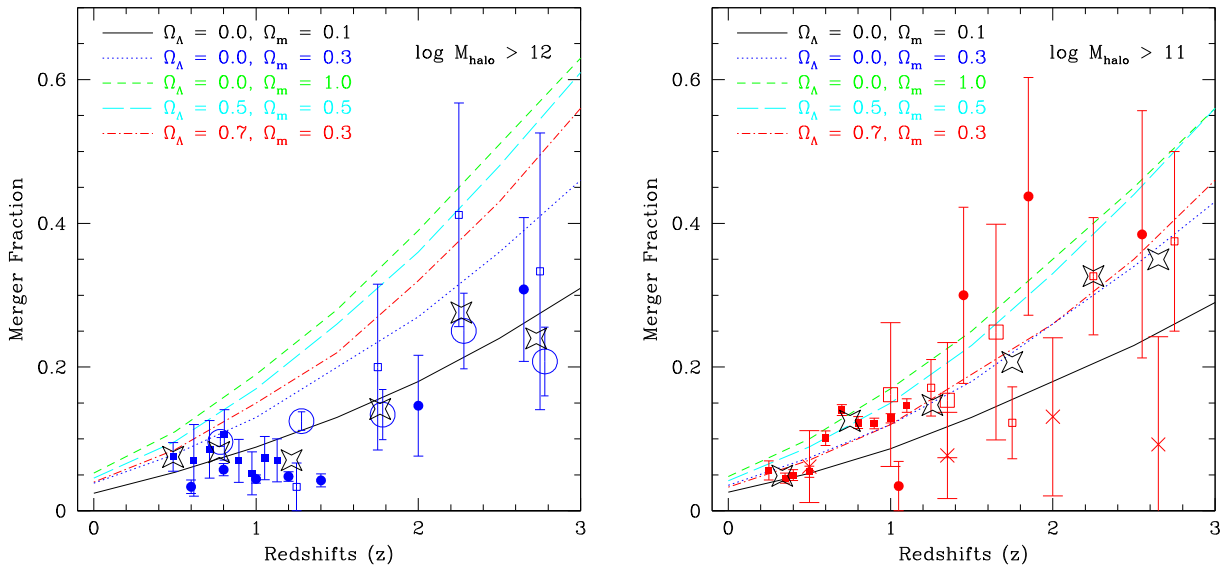

Figure 8. The halo merger histories compared with data for (a) haloes with masses $M_{\rm halo} > 10^{12}$ $M_\odot$ and (b) haloes with masses $M_{\rm halo} > 10^{11}$ $M_\odot$. The various lines show how the merger history varies with redshifts for haloes of this given mass, and using the cosmologies listed in the upper left. The solid symbols with errors bars are data on the merger fraction evolution taken from Conselice et al. (2009) for those at $z < 1.5$, merger fractions from pairs from the UDS (circles with inner error bars) and from Bluck et al. (2009) for $z > 1.5$ in panel (a) – all selected to have $M_* > 10^{11}$ $M_\odot$. For panel (b) the solid symbols with errors bars are taken from Conselice et al. (2009) for those at $z < 1.5$ and from Conselice et al. (2008) for $z > 1.5$, all selected to have $M_* > 10^{10}$ $M_\odot$. For both, the open symbols are from asymmetries from Mortlock et al. (2013) using CANDELS data. The average error weighted values of the merger fractions from the various surveys are shown as open black stars.

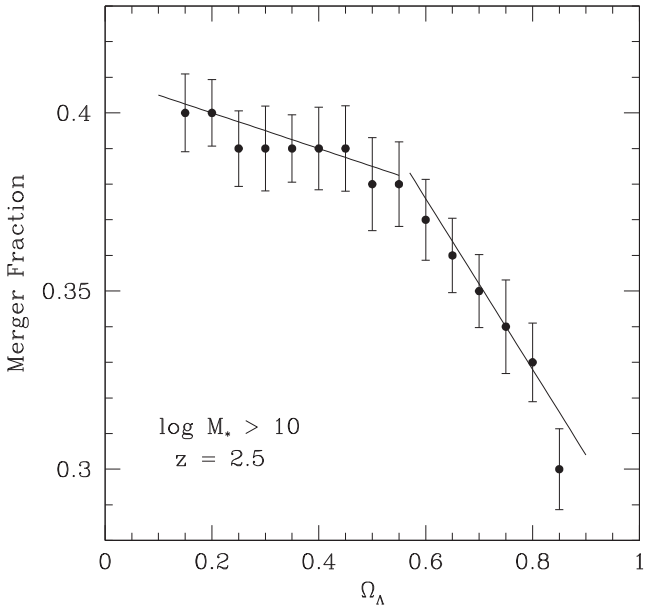

Figure 9. The relationship between the value of Ω_Λ and the resulting merger fraction for systems with stellar masses $>10^{10}$ $M_\odot$ at $z = 2.5$. This is for the condition such that $\Omega_\Lambda + \Omega_m = 1$. The solid lines are the best-fitting relationship for this relationship as described in the text.

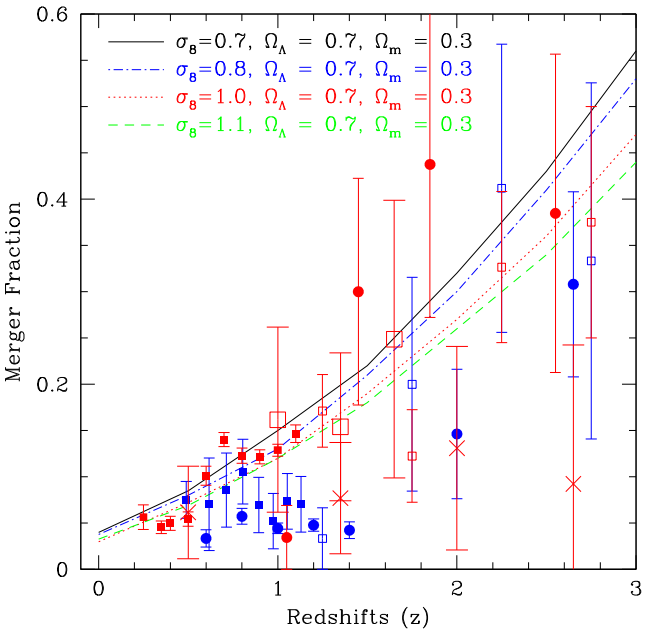

Figure 10. The evolution of the halo merger fraction for haloes with $M_{halo} > 10^{12}$ $M_\odot$ as a function of the value of σ_8 as in Fig. 3 except that here we show a comparison to data. The range shown is from $\sigma_8 = 0.7$ to $\sigma_8 = 1.1$, The points shown here are actual measures of the merger fraction for galaxies as a function of redshift. The red points are for $M_* > 10^{10}$ $M_\odot$ galaxies, including results from Conselice et al. (2003) at $z > 1$ in the HDF (solid circles); Conselice et al. (2009, solid boxes at $z < 1.2$) and Mortlock et al. (2013, small open boxes at $z > 1$). Also shown are pair merger fractions at separations of <30 kpc: Man et al. (2012, crosses at $z > 1$); Lopez-Sanjuan et al. (2010, large open boxes). The blue points show the merger history for $M_* > 10^{11}$ $M_\odot$ systems including results from Conselice et al. (2009, solid boxes at $z < 1.2$); Bluck et al. (2009, 2012, solid circles at $z > 0.5$) and Mortlock et al. (2013, open boxes at $z > 1$).

We can also now compare the merger history to the predicted halo mergers with differing values of the σ_8 parameter. Fig. 10 shows this comparison of our merger histories from observed galaxies in comparison to the halo mergers for differing values of σ_8. What we find is a relatively high value of the merger fraction in comparison to the halo merger histories. This suggests that the value of σ_8, as derived from our observations, would be low, with the value of $\sigma_8 = 0.7$ in best agreement with our observations. In the next subsections, we discuss how to use observed mergers as a competitive tool to constrain cosmology.

5.3 Cosmologies with an evolving equation of state

In the previous sections, we investigate the merger history and how it compares to dark matter halo mergers for a variety of cosmologies. However, it is clear that the concordance cosmology is the most likely cosmology with the large amount of supporting observations in the past few decades. What is not known for certain is the role of an evolving form of the dark energy, and how this may affect the galaxy formation process. In this section, we investigate how the merger history for haloes changes for a variety of evolving equations of states of the universe itself.

In fact, one of the major goals in cosmology is to constrain the equation of state of the universe, which relates the pressure (P) and density (ρ) of the dark energy, or $\omega = P/\rho$. The value of $\omega = -1$ is for a cosmological constant. The best current estimates of ω give values $\omega = -1.08 \pm 0.08$ (Anderson et al. 2012). The dark energy equation of state can also be written as $\omega(z) = \omega_0 + \omega_a(1 - a)$, although the measurements of the parameters ω_0 and ω_a are not well constrained, with the latest measurements giving $\omega_0 = -0.905 \pm 0.196$ and $\omega_a = -0.98 \pm 1.09$ (Sullivan et al. 2011).

In this section, we investigate how the merger history varies with different values of the equation of state of the universe. These merger predictions are from the GALACTICUS models of Benson (2012) using the equations from Percival (2005). First, we evaluate how the merger fraction varies for haloes with masses $M_{halo} > 10^{11}$ $M_\odot$ for values of ω between $\omega = -0.33$ and $\omega = -1.2$ (Fig. 11), with $\omega_a = 0$ for both. We also investigate this at two different halo masses, those with log $M_{halo} > 11$ and for log $M_{halo} > 12$. This shows a couple of interesting features regarding how the values of ω influence the halo merger history. We make the note that, as clearly shown in Fig. 11, it will be very difficult to utilize this type of figure to constrain the value of ω with galaxy merger histories given that there is not a large range of values of the halo merger fraction at different redshifts.

However, there are a few trends we can see. The first is that higher negative values of the equation of state parameter, ω, gives a higher merger fraction down to $z = 1.4$. However, at redshifts lower than this the models become nearly indistinguishable from one another. Furthermore, as in the basic merger history, the higher mass systems have higher merger fractions.

These changes in the different ω merger histories are well fit by a power law of the form $(1 + z)^m$ up to $z = 3$ (Table 4). We can use this to investigate the likelihood of being able to detect a difference in the merger history which may help constrain cosmology. We find that the difference between the effective merger histories is roughly $\delta f_{halo} \sim 0.005$ from values of $\omega = -0.9$ to $\omega = 1.1$. We discuss how this could be useful in cosmological investigations in Section 6.

We also investigate how the merger history varies with an evolving form of the equation of state, such that

$$\omega(z) = \omega_1 + \omega_a(1 - a), \quad (17)$$

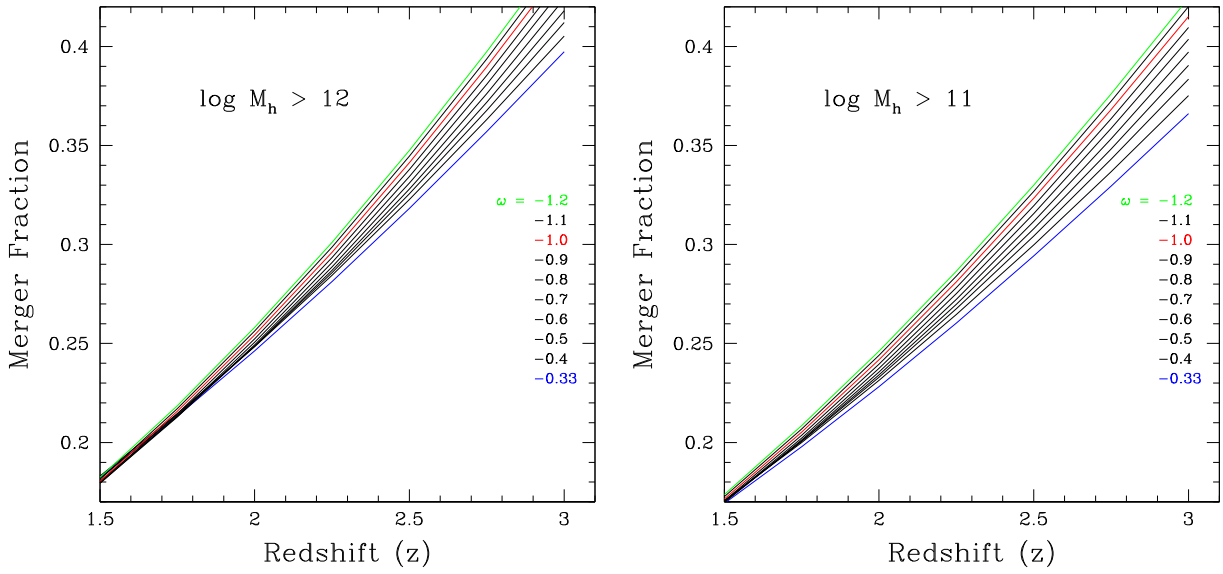

Figure 11. The change in the halo merger fraction as a function of redshift for differing values of the cosmological constant, as given in the equation of state for the dark energy, ω (Section 5.3). The left-hand panel shows the merger history for haloes of masses log $M_{\rm halo} > 12$, while the right is for haloes of mass log $M_{\rm halo} > 11$. The green line and blue lines show the range of our probe from $\omega = -1.2$ down to $\omega = -0.33$. The red line shows the values for the fiducial $\omega = -1$.

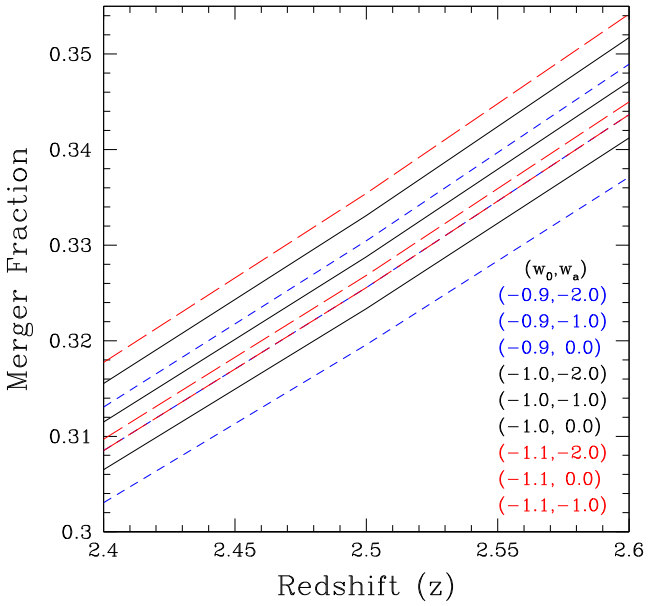

Figure 12. The relationship between the merger history as a function of redshift and different values of ω_0 and ω_1 for an evolving form of the dark energy equation of state (see Section 5.3).

where there is currently very little constraint based on observations of supernova (Sullivan et al. 2011). We however find that the merger histories for all reasonable combinations of ω_1 and ω_a are very close to one another in merger space (Fig. 12), such that the differences in $\delta f_m \sim 0.005$, again close to the accuracy needed to probe similar realistic differences for different constant ω values. This however becomes larger at higher redshifts such that the difference between different values for varying equations of state is highest. In the future, observing the merger fraction at $z \sim 6$ will be a major way to make this distinction using the ELTs and the JWST.

Table 5. How galaxy observables change as a function of cosmology, most notably the angular size distance and the luminosity distance, which has a direct effect on the measured stellar masses. Shown here is the ratio of the angular size distance, defined as the angular size distance at the given cosmology divided by the angular size distance in the concordance cosmology. Likewise the stellar mass differences between these two cosmologies is shown.

Ω_Λ	$\Omega_{\rm m}$	Ang. size dist ratio	ΔM
0.7	0.3	1.0	0.00
0.0	0.1	1.4	0.67
0.0	0.3	1.2	0.17
0.0	1.0	0.9	−0.10
0.5	0.5	1.1	0.09

5.4 Effects of cosmology on observables

One of the issues that we have to address when comparing galaxy observables, such as the merger history to models of varying cosmologies, is that the observables we use depend on the cosmology assumed when calculating derived values such as the stellar mass or merger rate. For example, the mergers we find are based on measuring a stellar mass and the value of this stellar mass can change depending on the cosmology used to calculate it.

Other features which change with cosmology are the physical separation between two galaxies, and whether or not this is a physical pair according to our definition based on the angular size distance. We therefore investigate in this section how the observed merger fractions and pairs can depend upon the cosmology assumed. We investigate these differences in terms of the concordance cosmology.

We show in Table 5 the values of the difference in derived stellar mass ΔM_* within the various cosmologies in reference to the coordinate cosmology. The biggest change is that at a given stellar mass selection, the galaxies examined are up to $\delta M_* = 0.67$ more massive depending on the cosmology examined. Likewise, we find that the

angular scale can vary by 40 per cent, but mostly around 20 per cent for cosmologies different from the concordance cosmology.

We investigate how the merger fraction changes when the measurements of stellar masses and galaxy separations are affected by different cosmologies. Note that the cosmology has more of an effect on the measurements for mergers which are found within pairs of galaxies. For morphological mergers, there is no angular separation to worry about and thus it is only the change in the distance modulus with cosmology that affects the choice of which bin a galaxy belong in.

For this reason, we utilize merger fractions, $f(M_*)$ which are a pure observable, as a function of stellar mass, which is as noted a function of the cosmology. We could use merger rates, but the timescales for these merger rates depends to some degree on cosmology, and on the nature of the dark matter. By using merger fractions, we are able to side-step this issue to some degree as it is a purely observational quantity.

To understand this issue, we examine how the merger fraction varies with pairs when changing the cosmological parameters, which results in the different selections of underlying haloes. We find that the observed merger fractions increase at larger separations, as long noted in pair studies of galaxies, and increases for higher mass selections at $z > 2$.

The result of this is that the cosmology with a low matter density, those with $\Omega_{\rm m} = 0.1$, $\Omega_\Lambda = 0$ will sample at a given angular separation, and a given flux cut lower mass galaxies and smaller separations as both the luminosity distance and angular size distance is larger in this cosmology than in the concordance one. To account for this cosmology, we would have to examine intrinsically fainter galaxies and look for pairs which have a smaller angular separation on the sky to match the intrinsic conditions used to find mergers in the coordinate cosmology. Both of these effects will decrease the merger fraction measured. If we take the $\Delta M = 0.67$ mass difference and the factor of 1.4 larger angular size separation, we would measure the merger fraction as $\delta f_{\rm m} \sim 0.05$ lower than what is plotted on Fig. 8. This is within the errors of the merger fractions themselves, but would decrease the measurement towards the model values further than the observed.

Likewise, universe's with a high mass density, i.e. with $\Omega_{\rm m} = 1$ have smaller angular size and luminosity distances. Therefore at a given flux, and at a given angular size measure on the sky, the galaxies sampled within this cosmology will be of lower mass and larger intrinsic separations. This gives the opposite effect from above, and to measure the correct merger fraction would require going to brighter systems and at larger angular separations. These both would result in a higher merger fraction based on measurements of how the observed merger fraction changes at fainter limits and smaller separations. We calculate for this cosmology that the true comparison merger fraction would be $\delta f_{\rm m} \sim 0.05$ higher, which would approach the higher values of the models, but would still be far from matching better than the concordance cosmology. More detailed comparisons will therefore have to be carefully done and all merger fractions measured in the cosmology being compared with.

There is also the issue that our mapping of stellar and halo masses will depend on the cosmology assumed in the calculation. We show these different stellar versus halo masses using different cosmologies in Fig. 13. For the concordance cosmologies with differing values of σ_8 from 0.7 to 0.9, there is a variation of the total mass for a halo mass at $\log M_* \sim 11$ of 0.3 dex. This would thereafter lead to a change in the derived merger fraction by at most 10 per cent. As can also be seen, there is a large change in the measurement of the mass relations for the cosmologies with $\Omega_{\rm m} = 0.1$ and $\Omega_{\rm m} = 1$. These differences lead to a factor of 10 difference in the halo mass at a given stellar mass from the concordance cosmology at masses around $\log M_* \sim 11$ in the most extreme examples. However, as the halo merger fraction dependence on mass is quite shallow, this only leads to an addition small uncertainty in the halo merger fraction of $f_{\rm halo} \sim 0.025$.

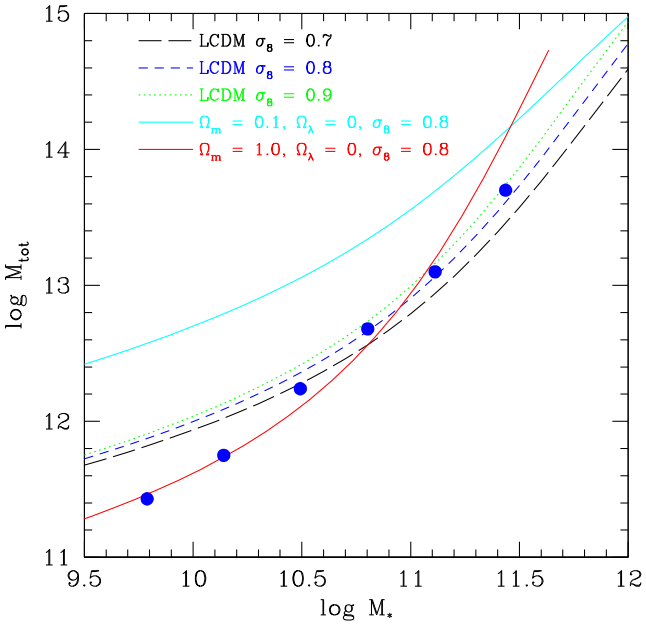

Figure 13. The stellar mass and total mass relation using the abundance matching methodology described in Section 5.1, but using different cosmologies within the calculation for the relations at $z = 1$–1.5. The dashed lines are for the concordance cosmology but using different values of σ_8. The solid lines are for $\Omega = 1.0$ (red) and $\Omega_{\rm m} = 0.1$ (cyan), with both at $\Omega_\Lambda = 0$. The blue points are the kinematic relations for the concordance cosmology described in Section 5.1.

When better merger fractions are available they can be measured in different cosmologies and thereby produce a more detail comparison between models and data. In practice, this will consist of calculating stellar masses and galaxy merger fractions at the different cosmologies under study. This should not be complicated to do, only time intensive. We finally note that the use of morphology and structure to find galaxies merging is potentially a more powerful approach than those from pairs of galaxies. The reason is there is less effects from cosmology on the measures due to only the stellar mass selection being affected since there is no selection by angular separation of two galaxies.

6 DISCUSSION

6.1 Mergers as a cosmological tool

In this sub-section, we investigate using the merger history as a cosmological tool. We preface this by stating that mergers may never be as good of a method as some to measure cosmological properties. The reason that methods that use standard candles such as Type Ia supernova are so successful is that fundamentally there are only two observations – the flux and redshift, which can then be compared directly to cosmological predictions. However, our method does allow us to measure cosmology by the effect it has on objects within the universe, rather than its effects of the expansion which most methods use.

The use of the galaxy merger history as a competitive cosmological tool will require that we know more about the properties of galaxies, namely accurate measurements of galaxy masses and the ability to understand the merger history without significant systematic biases. Although the merger history has some agreement using different methods such using galaxy pairs and through morphology (e.g. Conselice et al. 2009; Lotz et al. 2011), there still remains work to be done to determine whether or not we can actually measure the merger fraction or merger rate to within 1 per cent up to $z \sim 3$. This means that we will have to measure the merger history accurately over all environments, such that the effects of cosmic variance produces less than a 1 per cent systematic error on the measured merger values.

Even if we can measure the merger history accurately without significant systematic errors, there is still the issue of shot noise within these measurements, requiring larger area surveys than what we currently have. We can investigate how good our merger fraction measurements will need to be to measure the history of mergers to distinguish between cosmological models.

To measure accurately the differences in the cosmological models presented in this paper requires that the accuracy in measuring merger fractions for galaxies at a given mass is $\delta f_{\rm m} \sim 0.01$. To distinguish between $\delta f_{\rm m} \sim 0.01$, for a merger fraction of $f_{\rm m} \sim 0.3$, i.e. a 30 per cent fraction of the population undergoing mergers, which we see at $z > 2$ at high stellar mass, we need to measure accurately the merger fraction over 4335 arcmin^2 or 1.2 deg^2. Surveys this large do now exist, such as the CFHT legacy survey and the UKIDSS UDS, and the next generation of photometric and spectroscopic redshifts within these should make an attempt at measuring merger fractions by using pairs. However, the use of morphology for the measurement of merger fractions will be difficult given that only a very small fraction of this area has been imaged at high enough resolution in the near-infrared in the CANDELS survey (e.g. Grogin et al. 2011; Koekemoer et al. 2011).

We can further investigate the accuracy we need to get a 3σ accuracy on statistical measures of merger fractions. If we want to obtain a 3σ measurement at $\delta f_{\rm m} \sim 0.01$, we will need a larger area of 8.1 deg^2. This is much larger than any deep surveys, yet in the future, those with *Euclid* or WFIRST will be able to measure the structure/morphologies over this area.

Attempting to use the merger history for measurements of different values of the equation of state parameter, ω, and for an evolving form of $\omega(z)$, require a precision about twice as good. As briefly discussed in Section 5.3, to measure different merger histories that can constrain between small values of ω to within ± 0.1 around $\omega = -1$, or to constrain better than current estimates of ω_1 and $\omega_{\rm a}$ requires that we measure the merger fraction to within $f_{\rm halo} \sim 0.005$ or better. This will require deep surveys of at least 2.5 deg^2 in area, which is currently possible by combining existing surveys. To obtain 3σ statistical errors will require an area of $\sim$17 deg^2. This also assumes that other errors, such as systematics with redshifts, stellar masses, etc. are small, which they are not. Alongside obtaining deeper and wider surveys we will also need to be more certain that accurate stellar masses and photometric/spectroscopic redshifts can be measured. As these improve to measure galaxy evolution so will our ability to use galaxies as a cosmological tool.

6.2 Implications

There are a few important implications within our results, for cosmology, structure assembly, galaxy formation, as well as for our ability to measure the merger history. We briefly detail these here, although a further analysis of these will be addressed in later papers. The first issue is that by examining the dark matter assembly itself, rather than relying on the baryonic physics behind semi-analytical simulations we get much better agreement with the merger data, making reasonable assumptions about the relation between the observed stellar mass of galaxies and their total halo mass from known scaling relations. This is an important point to make, as it reflects the well-known problem of matching the abundances of galaxies with their total halo mass functions. It is clear that the galaxy mass function has a shape which differs significantly from the predicted halo mass function and processes such as feedback, photoionization, conduction, gas cooling among other baryonic processes must be implemented to correctly model the observed galaxy mass function (e.g. Benson et al. 2003).

However, for whatever reason the implementation of the baryonic physics in semi-analytical models does not accurately reproduce the merger fraction and rate history of galaxies. This implies that the baryonic physics implemented in these models is missing ingredients necessary to reproduce the observed history of galaxy assembly, or is implementing them in an incorrect way. This is perhaps also reflected in the problem of semi-analytical models in predicting the number of massive galaxies at high redshift (e.g. Conselice et al. 2007; Guo et al. 2011). While the WDM models do better, this may reflect less structure on smaller scales, and thus more likely to produce similar mass mergers.

We also demonstrate that the merger history depends on cosmology such that cosmologies with higher matter densities will contain a high merger fraction and rate, and therefore that there will be more massive haloes in these cosmologies found in the nearby universe. We furthermore show, in a limited way, that there is also good agreement between the merger history and the generally accepted cosmological model, such that $\Omega_{\rm m} = 0.3$ and $\Omega_\Lambda = 0.7$ is the best-fitting model based on a wide range of possible cosmologies. However, it is worth pointing out that this constraint is not very useful in itself given that the standard model of cosmology is generally accepted. To be a useful indicator for cosmology, this method would have to be able to distinguish suitable differences in the merger history for the limited range of cosmologies that are now predicted in CMBR experiments such as *WMAP* and *Planck* (e.g. Komatsu et al. 2011; Ade et al. 2013). However, it is reassuring that the agreement we find demonstrates a consistency between the dominant and generally accepted cosmology, and how the dark matter on the level of galaxies is assembling through mergers.

It is possible to distinguish between various cosmologies with various $\Omega_{\rm m}$ and Ω_Λ values; however, we conclude that the accuracy in the merger fraction needed to do this is very high, of the order of 1 per cent to distinguish between various cosmologies with similar values. This will require surveys from 1.2 deg^2 in area up to 20 deg^2, but the real challenge will be in making sure that all systematics are accounted for when carrying out this comparison. One of these challenges is understanding the merger time-scale, that is how long an asymmetric galaxy, or a galaxy seen in a pair, takes to merge. This is essential when comparing with any predictions. The merger time-scale is estimated to be 0.4 Gyr in this paper, which is what is found empirically by observing the change in the observed merger fraction (Conselice 2009), as well as an average over simulations (e.g. Conselice 2006; Lotz et al. 2010a). However, the merger time-scale does depend upon the galaxy gas mass fraction (e.g. Lotz et al. 2010a) and other properties such as viewing angle, bulge-to-disc ratio and orbital type. While the average of such properties may be calculable from models, it remains to be determined whether time-scales seen at high redshift are similar

to those predicted in models. Future detailed simulations with for example *Eagle* and *Illustris* will help reveal time-scales for these mergers which will eliminate another key systematic to create these comparisons.

To avoid the time-scale issue completely, the merger fraction comparison could be carried out using galaxies within close pairs – i.e. systems which are just about to merge. Simulations can predict this often as well as they can an actual merger, and observationally, these pairs are not as ambiguous at times as deciding if a galaxy is an active merger or not. Likely, a combination of pre-merger close pairs and post-merger morphological signatures are best used together as a check on systematics of both methods.

We also note that the agreement with the theory for some of our merger histories is not perfect. The most obvious case of this is the comparison between the halo merger history and galaxy mergers selected with stellar masses $M_* > 10^{11}$ $M_\odot$ (Fig. 8). Here, we can see that at $z < 1$ the galaxy merger history is significantly less than that predicted based on the halo mergers. This is likely an indication that we are simply not detecting all the mergers for this population of very massive galaxies at this epoch. The reason for this is that many of these massive galaxies are fairly red at this epoch, and any mergers would be 'dry' and thus not be detectable within the CAS systems, from which these $z < 1$ values are measured (e.g. Hernandez-Toledo et al. 2006). What is needed is a full analysis of the merger history at this mass range using galaxies in kinematic pairs, as well as through clustering analyses to determine the actual merger rate.

It is likely that the ultimate measurement of the merger history will be carried out through a mixture of galaxies in pairs, and those measured through their high asymmetries. Typically, the morphological approach is useful at higher redshifts, while the pair method is more suitable for lower redshift galaxies, especially at $z < 1$ where there are significant investments in spectroscopy within deep fields.

7 SUMMARY

This paper explores the idea of using galaxy mergers as a probe of cosmology. While the idea that galaxy merging can be used to probe the properties of the universe is not new (e.g. Carlberg 1991), the use of it as a cosmological probe has never been fully characterized, or explored. In this paper, we have shown that using a variety of assumptions regarding how the halo merger history can be matched to some degree with the galaxy merger history, the current observations of the galaxy merger history are in relative agreement with a concordance cosmological model.

Our other major findings are as follows.

(1) The halo merger history varies as a function of halo mass, such that systems with larger halo masses have higher merger fraction at all redshifts. This is in direct contrast to the observations of galaxy mergers whereby the most massive systems (as measured in stars) have a higher merger fraction at $z > 2$, but tend to show little merging at later times.

(2) Semi-analytical models based on CDM from the Millennium simulation underpredict the galaxy merger history, but that those using WDM with a particle temperature of ∼1 keV do a better job in predicting the merger history than a CDM semi-analytical model.

(3) The merger history of haloes varies significantly with cosmology. The merger fraction and history are lower for lower matter density Ω_m cosmologies, and highest for cosmologies where $\Omega_m = 1$. The difference between these is large, around $\delta f_{halo} \sim 0.25$ at $z \sim 3$ and easily distinguishable with current measurements.

(4) We show that it is possible to compare haloes to galaxies through the use of halo mass to stellar mass calibrations, and thus to compare directly halo mergers to galaxy mergers. When comparing the available data to these models the best fit is a concordance cosmology with $\Omega_\Lambda = 0.7$ and $\Omega_m = 0.3$. We also show how the merger fraction varies as a function of Ω_Λ at a single redshift, $z = 2.5$, and how this can be further used to calculate the best-fitting value of $\Omega_\Lambda = 0.84^{+0.16}_{-0.17}$

(5) The halo merger history is also strongly dependent on the value of σ_8, such that lower values of σ_8 give a higher merger fraction.

(6) We also examine how the merger history changes for differing values of the dark energy equation of state ω, and how a varying $\omega(z)$ changes the calculated halo merger history. We find that accurate merger fractions on the level of $\delta f \sim 0.005$ are required to distinguish between competing models. The difference between the predictions for the merger histories is highest at the highest redshifts and in the future JWST and the E-ELT can provide these measurements.

The use of the galaxy merger history to probe cosmology in a competitive way with other techniques such as supernova, baryonic acoustic oscillations and CMBR work will require several improvements. The first is that we must be able to match better the stellar masses of galaxies and their halo masses, as well as have a firmer idea of the mass ranges that produce merging and the time-scale for halo mergers, and how these relate to the time-scale for galaxy mergers. While halo occupation is one way to do this, and can produce successfully matched merger histories, we are able to derive similar results using a calibration based on the kinematics of galaxies.

Overall, we find that the accuracy of merger fractions would have to exceed $\delta f_m \sim 0.01$ to be able to differentiate between current uncertainties in the value of cosmological parameters. As explained in this paper, this will required surveys on the sky of area up to several 10 deg^2. These types of surveys must also have accurate stellar masses and reliable redshifts with uncertainties, along with the merger uncertainties, which do not add up to a merger fraction errors that are larger than 1 per cent. This will be difficult, but by combining results at various redshifts, and various masses, some of these limits on uncertainties could be relaxed a bit and systematics better understood. Future surveys such as *Euclid* and LSST will be ideal for carrying out this type of analysis and has a potential to be competitive with other techniques such as those listed above.

ACKNOWLEDGEMENTS

We thank Mike Santos, Aisyah Sahdan and Jack Johnson for their early contributions to this work, and Ed Copeland for illuminating discussions. CJC, AM and AFLB acknowledge support from the STFC and the Leverhulme Trust. DP acknowledged the support of an Australian Post-graduate Award and an Endeavour Research Fellowship. AFLB acknowledges support from NSERC (National Science and Engineering Research Council) of Canada.

REFERENCES

Ade P. et al., 2013, preprint (arXiv:1303.5076)
Ade P. et al., 2014, Phys. Rev. Lett., 112, 241101

Allen S. W., Schmidt R. W., Ebeling H., Fabian A. C., van Speybroeck L., 2004, MNRAS, 353, 457
Anderson L. et al., 2012, MNRAS, 427, 3435
Benson A., 2012, New Astron., 17, 175
Benson A. J., Bower R. G., Frenk C. S., Lacey C. G., Baugh C. M., Cole S., 2003, ApJ, 599, 38
Bertone S., Conselice C. J., 2009, MNRAS, 396, 2345
Bertone S., De Lucia G., Thomas P. A., 2007, MNRAS, 379, 1143
Blake C. et al., 2011, MNRAS, 418, 1707
Bluck A. F. L., Conselice C. J., Bouwens R. J., Daddi E., Dickinson M., Papovich C., Yan H., 2009, MNRAS, 394, L51
Bluck A. F. L., Conselice C. J., Buitrago F., Grutzbauch R., Hoyos C., Mortlock A., Bauer A. E., 2012, ApJ, 747, 34
Bower R. G., Benson A. J., Malbon R., Helly J. C., Frenk C. S., Baugh C. M., Cole S., Lacey C. G., 2006, MNRAS, 370, 654
Bruzual G., Charlot S., 2003, MNRAS, 344, 1000 (BC03)
Bundy K. et al., 2006, ApJ, 651, 120
Carlberg R. G., 1991, ApJ, 37, 429
Conroy C., Wechsler R. H., 2009, ApJ, 696, 620
Conselice C. J., 2003, ApJS, 147, 1
Conselice C. J., 2006, ApJ, 638, 686
Conselice C. J., 2009, MNRAS, 399, L16
Conselice C. J., 2014, ARA&A, preprint (arXiv:1403.2783)
Conselice C. J., Arnold J., 2009, MNRAS, 397, 208
Conselice C. J., Bershady M. A., Dickinson M., Papovich C., 2003, AJ, 126, 1183
Conselice C. J., Blackburne J., Papovich C., 2005, ApJ, 620, 564
Conselice C. J. et al., 2007, MNRAS, 381, 962
Conselice C. J., Rajgor S., Myers R., 2008, MNRAS, 386, 909
Conselice C. J., Yang C., Bluck A. F. L., 2009, MNRAS, 394, 1956
Conselice C. J. et al., 2011, MNRAS, 413, 80
Conselice C. J., Mortlock A., Bluck A. F. L., Grutzbauch R., Duncan K., 2013, MNRAS, 430, 1051
De Lucia G., Springel V., White S. D. M., Croton D., Kauffmann G., 2006, MNRAS, 366, 499
De Propris R. et al., 2010, AJ, 139, 794
Eisenstein D. J., Hu W., 1999, ApJ, 511, 5
Eisenstein D. J. et al., 2005, ApJ, 633, 560
Fakhouri O., Ma C.-P., 2008, MNRAS, 386, 577
Fakhouri O., Ma C.-P., Boylan-Kolchin M., 2010, MNRAS, 386, 577
Foucaud S., Conselice C. J., Hartley W. G., Lane K. P., Bamford S. P., Almaini O., Bundy K., 2010, MNRAS, 406, 147
Gottlober S., Klypin A., Kravtsov A. V., 2001, ApJ, 546, 223
Grogin N. et al., 2011, ApJS, 197, 35
Guo Q. et al., 2011, MNRAS, 413, 101
Hamilton A., 2001, MNRAS, 322, 419
Hartley W. G. et al., 2013, MNRAS, 431, 3045
Hernandez-Toledo H. M., Avila-Reese V., Salazar-Contreras J. R., Conselice C. J., 2006, AJ, 132, 71
Hopkins P. F. et al., 2010, ApJ, 724, 915
Hubble E., 1929, Proc. Natl. Acad. Sci. USA, 15, 168
Jenkins A. et al., 1998, ApJ, 499, 20
Jenkins A., Frenk C. S., White S. D. M., Colberg J. M., Cole S., Evrard A. E., Couchman H. M. P., Yoshida N., 2001, MNRAS, 321, 372
Jogee S. et al., 2009, ApJ, 697, 1971
Kessler R. et al., 2009, ApJS, 185, 32
Kneber A. et al., 2013, MNRAS, 435, 1618
Koekemoer A. M. et al., 2011, ApJS, 197, 36
Komatsu E. et al., 2011, ApJS, 192, 18
Lin L. et al., 2008, ApJ, 681, 232
Limber D. N., 1954, ApJ, 119, 655
Lopez-Sanjuan C. et al., 2010, ApJ, 710, 1170
Lotz J. M., Jonsson P., Cox T. J., Primack J. R., 2008a, MNRAS, 391, 1137
Lotz J. M. et al., 2008b, ApJ, 672, 177
Lotz J. M., Jonsson P., Cox T. J., Primack J. R., 2010a, MNRAS, 404, 575
Lotz J. M., Jonsson P., Cox T. J., Primack J. R., 2010b, MNRAS, 404, 590
Lotz J. M., Jonsson P., Cox T. J., Croton D., Primack J. R., Somverille R. S., Stewart K., 2011, ApJ, 742, 103
Maller A. H., Katz N., Keres D., Dave R., Weinberg D. H., 2006, ApJ, 647, 763
Man A. W. S., Toft S., Zirm A. W., Wuyts S., van der Wel A., 2012, ApJ, 744, 85
Mannucci F. et al., 2009, MNRAS, 398, 1915
Menci N., Fiore F., Lamastra A., 2012, MNRAS, 421, 2384
Moreno J., Bluck A. F. L., Ellison S. L., Patton D. R., Torrey P., Moster B. P., 2013, MNRAS, 436, 1765
Mortlock A., Conselice C. J., Bluck A. F. L., Bauer A. E., Grützbauch R., Buitrago F., Ownsworth J., 2011, MNRAS, 413, 2845
Mortlock A. et al., 2013, MNRAS, 433, 1185
Muzzin A. et al., 2013, ApJ, 777, 18
Percival W. J., 2005, A&A, 443, 819
Perlmutter S. et al., 1999, ApJ, 517, 565
Press W. H., Schechter P., 1974, ApJ, 187, 425
Reed D. S., Bower R., Frenk C. S., Jenkins A., Theuns T., 2007, MNRAS, 374, 2
Riess A. G. et al., 1998, AJ, 114, 722
Riess A. G. et al., 2004, ApJ, 607, 665
Sandage A., 1988, ARA&A, 26, 561
Seljak U., 2000, MNRAS, 318, 203
Sheth R. K., Tormen G., 1999, MNRAS, 308, 119
Springel V. et al., 2005, Nature, 435, 629
Stewart K. R., Bullock J. S., Barton E. J., Wechsler R. H., 2009, ApJ, 702, 1005
Sullivan M. et al., 2011, ApJ, 737, 102
Tinker J. L., Weinberg D. H., Zheng Z., Zehavi I., 2005, ApJ, 631, 41
Tinker J., Kravtsov A. V., Klypin A., Abazajian K., Warren M., Yepes G., Gottlober S., Holz D. E., 2008, ApJ, 688, 709
Tinker J. L., Robertson B. E., Kravtsov A. V., Klypin A., Warren M. S., Yepes G., Gottlober S., 2010, ApJ, 724, 878
Tolman R. C., 1930, Proc. Natl. Acad. Sci. USA, 16, 511
Turner M. S., Riess A. G., 2002, ApJ, 569, 18
Vikhlinin A. et al., 2009, ApJ, 692, 1060
White S. D. M., Rees M., 1978, MNRAS, 183, 341
Williams R. E. et al., 1996, AJ, 112, 1335
Zehavi I. et al., 2011, ApJ, 736, 59
Zheng Z. et al., 2005, ApJ, 633, 791

This paper has been typeset from a TEX/LATEX file prepared by the author.